



The Abdus Salam  
International Centre for Theoretical Physics



2256-7

**Workshop on Aerosol Impact in the Environment: from Air Pollution to Climate Change**

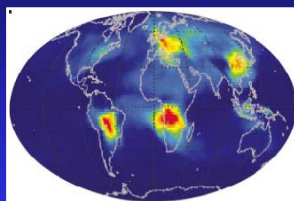
*8 - 12 August 2011*

**Development of aerosol retrieval: Applications in ground-based remote sensing**

O. Dubovik

*Lab. d'Optique Atmosphérique, Lille, France*

# Remote sensing of atmospheric aerosols:



Oleg Dubovik

*University of Lille 1, CNRS, France*

*NASA/GSFC, Greenbelt, USA*

## Part 1:

- ✧ **aerosol remote sensing and climate - overview**
- ✧ **remote sensing from ground: AERONET**
  - concept of retrieval;
  - aerosol model;
  - AERONET primary and secondary retrieval products
  - error estimations, sensitivity studies

## Part 1:

- ✧ **potential of remote sensing from space:**
  - aerosol monitoring using satellite imagers: **PARASOL**
  - synergy of remote sensing and modeling: **inverse modeling**

## **Microphysical properties:**

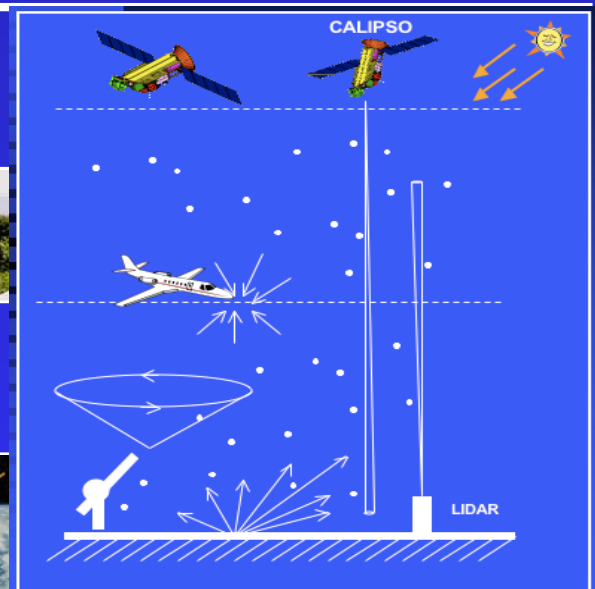
Concentration, sizes, composition, shapes, mixing, orientation, etc.



Theory of electromagnetic interactions of light with small particles, etc.

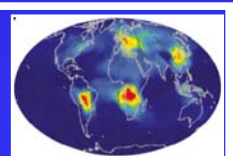
## **Remote sensing:**

- passive,
- active,
- satellite,
- ground-based,
- airborne,
- etc.

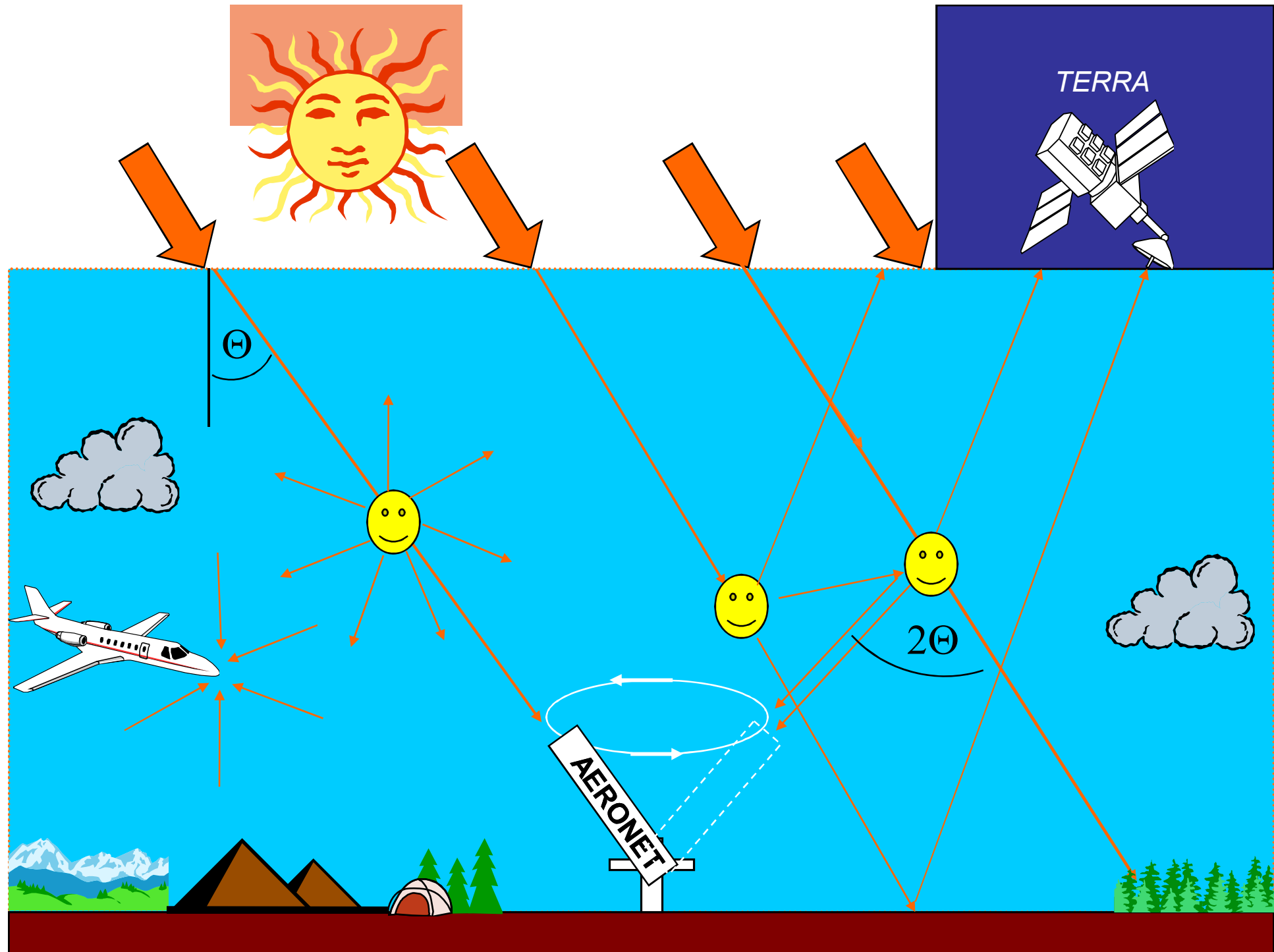


## **Geophysical:**

Spatial and temporal distributions of microphysical properties



**Climate, Environment, etc. :**  
Heating, Cooling, Air Quality, etc



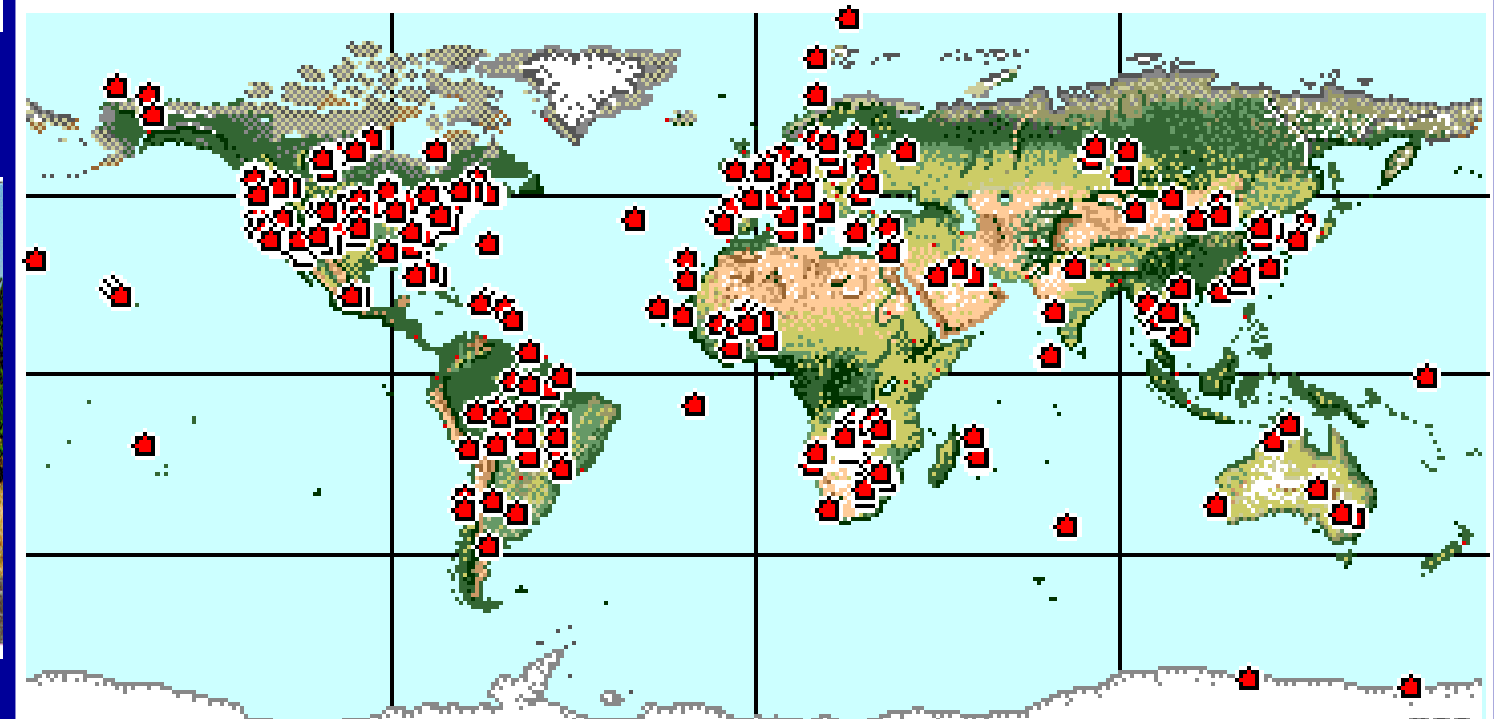


# AERONET (AErosol RObotic NETwork)-

An internationally Federated Network

1993-2003

CENTRE NATIONAL  
DE LA RECHERCHE  
SCIENTIFIQUE



- Characterization of aerosol optical properties
- Validation of satellite aerosol retrieval
- Near real-time acquisition; long term measurements
- Homepage access: <http://aeronet.gsfc.nasa.gov>



### Data Display Controls

AERONET Data Type:  AOT  Water Vapor  
AOT Level:  Level 1.0  Level 1.5  Level 2.0  
Data Format:  Daily averages  All points

Related Product Availability (select each day below):

- Show [Spherical](#) OR [Spheroid](#) Almucantars
- Show [Back Trajectories - Disclaimer](#)
- Show [MPLNET Images - Disclaimer](#)
- MODIS Images (Not available)
- Visible Satellite Images (Not available)

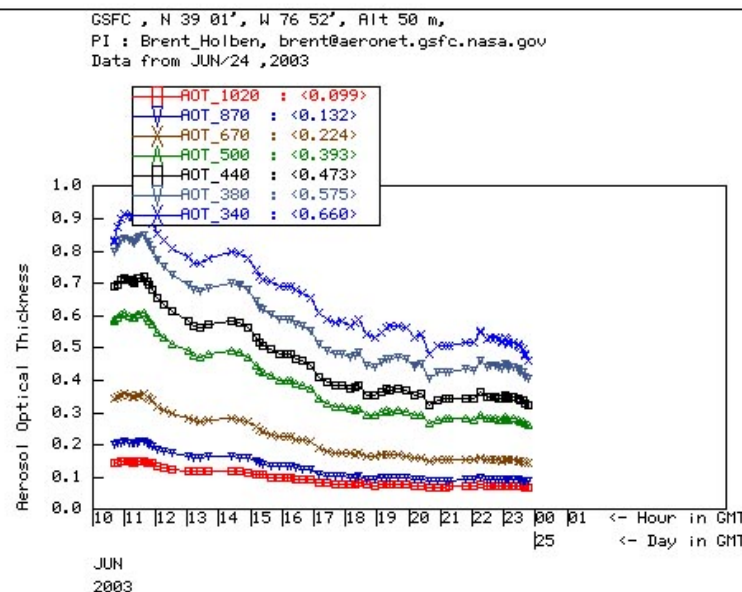
Choose year : [1993](#) [1994](#) [1995](#) [1996](#) [1997](#) [1998](#) [1999](#) [2000](#) [2001](#) [2002](#) [2003](#)

Choose month of 2003 : [JAN](#) [FEB](#) [MAR](#) [APR](#) [MAY](#) [JUN](#) [JUL](#) [AUG](#) [SEP](#)

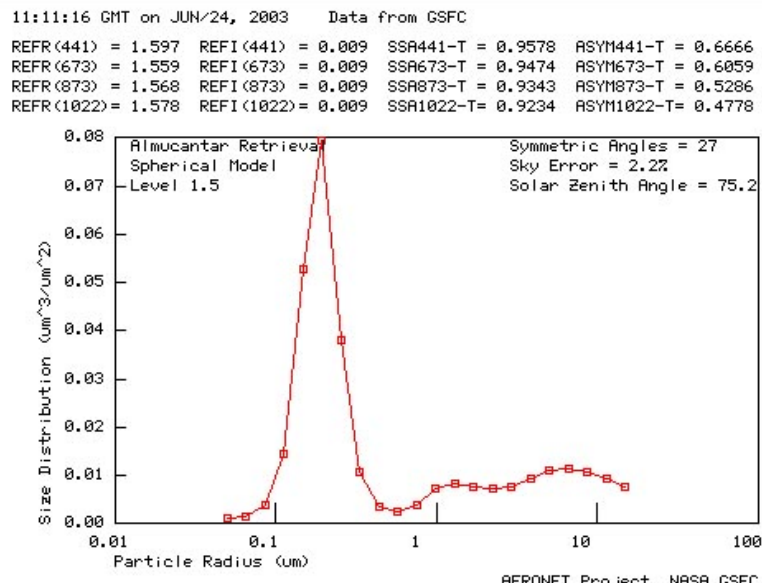
Choose day of JUN 2003

|                    |                    |                    |                    |                    |                    |                    |                    |                    |                    |                    |                    |
|--------------------|--------------------|--------------------|--------------------|--------------------|--------------------|--------------------|--------------------|--------------------|--------------------|--------------------|--------------------|
| <a href="#">1</a>  | <a href="#">2</a>  | 3                  | 4                  | <a href="#">5</a>  | <a href="#">6</a>  | 7                  | 8                  | <a href="#">9</a>  | <a href="#">10</a> | <a href="#">11</a> | <a href="#">12</a> |
| <a href="#">13</a> | <a href="#">14</a> | <a href="#">15</a> | <a href="#">16</a> | 17                 | <a href="#">18</a> | <a href="#">19</a> | <a href="#">20</a> | <a href="#">21</a> | 22                 | <a href="#">23</a> | <a href="#">24</a> |
| <a href="#">25</a> | <a href="#">26</a> | <a href="#">27</a> | <a href="#">28</a> | <a href="#">29</a> | <a href="#">30</a> |                    |                    |                    |                    |                    |                    |

### AOT Level 1.0 Data from JUN 24 of 2003



### Level 1.5 Spherical Model Almucantar Retrieval No 1 on JUN 24 of 2003



## Download Data for Capo\_Verde

Select the start and end time of the data download period:

START:

1 JAN 1994

END:

1 JAN 2003

[Data Descriptions](#)

[Data Units](#)

[Development Status](#)

[Update Log](#)

**Note:** Data are not available if the data type is *italicized*

Select the data type(s) with checkbox:

### Aerosol Optical Thickness\*:

1.  Level 1.0 (Raw)
2.  Level 1.5 (Cloud Screened)
3.  Level 2.0 (Quality Assured)

\*also WV and Angstrom Parameters

Select All AOT

### Raw Data (Calibration Applied):

4.  Almucantars
  5.  Polar Principal Planes
  6. *BRDF*
  7.  Principal Planes
- Select All Raw Data

### Nakajima Almucantar Retrievals

8.  SKYRAD.PAK

### Almucantar Retrievals

#### Total Only

9.  Size Distribution
10.  Refractive Index
11.  AOT Coincident

Select All Retrievals

#### Total/Fine/Coarse Modes

12.  Volume
13.  AOT Absorption
14.  AOT Extinction
15.  SSA
16.  Asymmetry Factor
17.  Phase Functions
18.  Combined Retrievals (9-16)

# AERONET Data Flows

<http://aeronet.gsfc.nasa.gov>

Flux measurements

Direct -  $\lambda=340, 380, 440, 500, 670, 870, 940, 1020$  nm

Diffuse -  $\lambda=440, 670, 870, 1020$  nm (alm, pp, pol)

Calibration and processing information

Aerosol optical depth and  
precipitable water computations

Cloud screening and quality control

Inversion products

Volume size distribution ( $0.05 < R < 15 \mu\text{m}$ ),  
refractive index, single scattering albedo  
( $\lambda=440, 670, 870, 1020$  nm), fraction of  
spherical particles

Holben et al.  
*RSE*, 1998  
Holben et al.  
*JGR*, 2001

Eck et al.  
*JGR*, 1999

Smirnov et al.  
*RSE*, 2000

Dubovik and King  
*JGR*, 2000  
Dubovik et al.  
*JGR*, 2000  
*GRL*, 2002, 2006

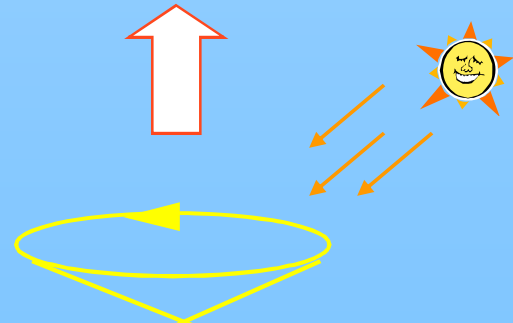
# AERONET Inversion

## Forward Model:

**Single Scat:** ensemble of polydisperse randomly oriented spheroids  
(mixture of spherical and non-spherical aerosol components)

**Multiple Scat:** (scalar) Nakajima and Tanaka, 1988, or  
(polarized) Lenouable et al., JQSRT, 2007

$\tau(\lambda), I(\lambda, \Theta), P(\lambda, \Theta)$



## Optimized Numerical inversion:

- Accounting for uncertainty ( $F_{11}; -F_{12}/F_{11}$  !!!)
- Setting a priori constraints



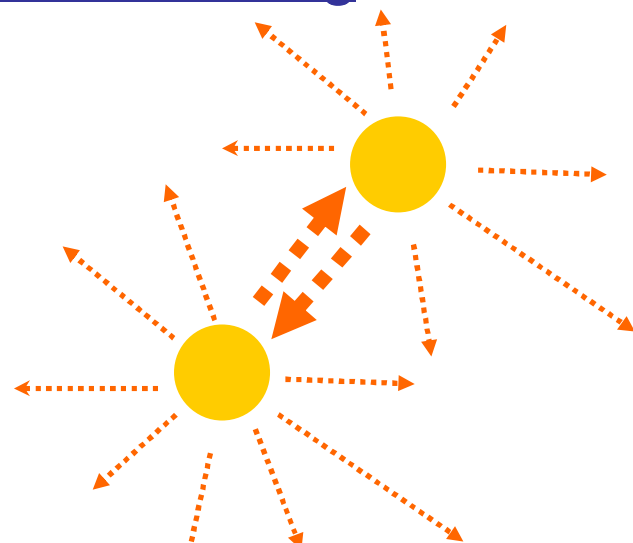
aerosol particle sizes,  
complex refractive index (SSA),  
Non-spherical fraction

# Multiple Scattering

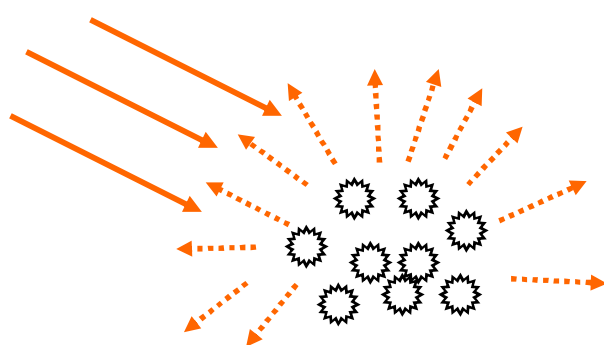
Multiple scattering effects are accounted by solving **scalar** or **vector**

radiative transfer equation accounting for **BRDF** or **BPRF** of surface reflectance

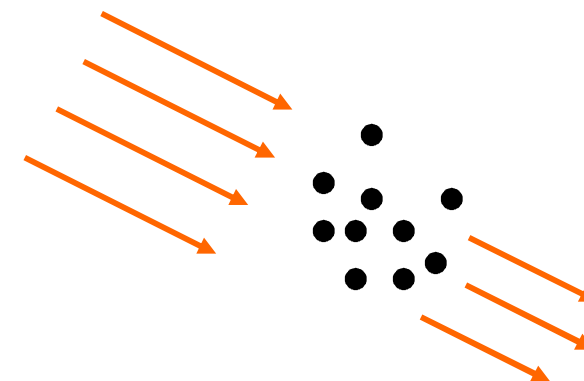
Aerosol scattering



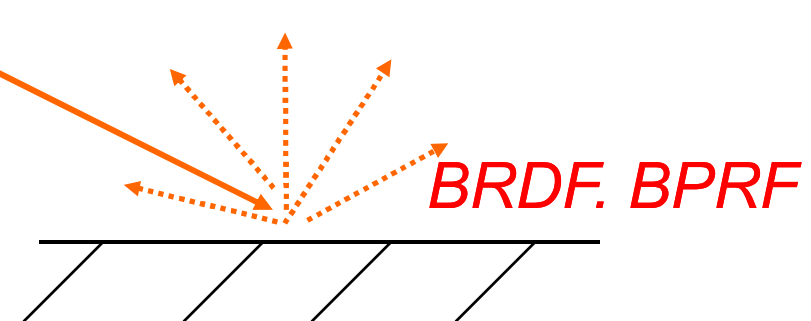
Molecular scattering



Gaseous absorption

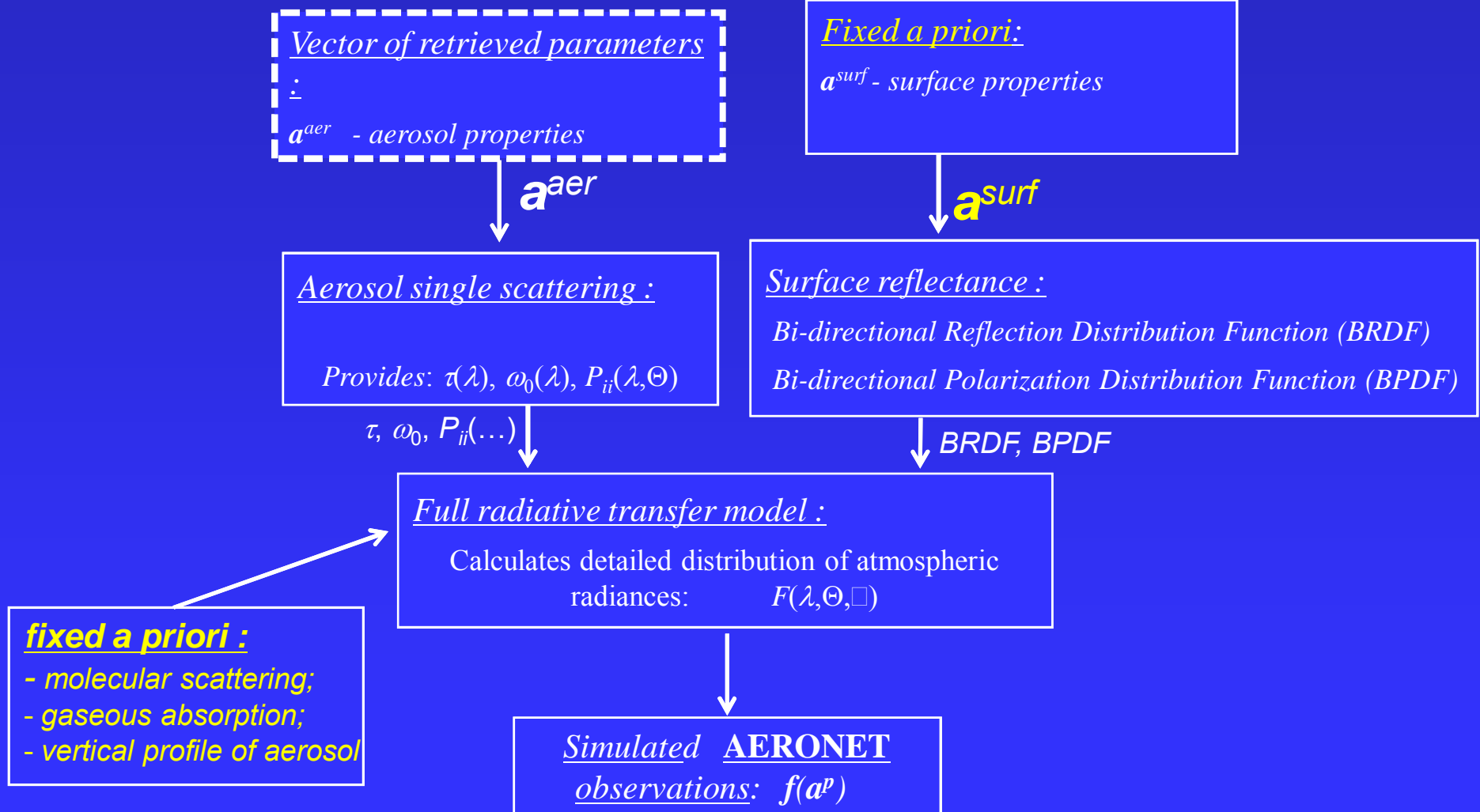


Surface reflection



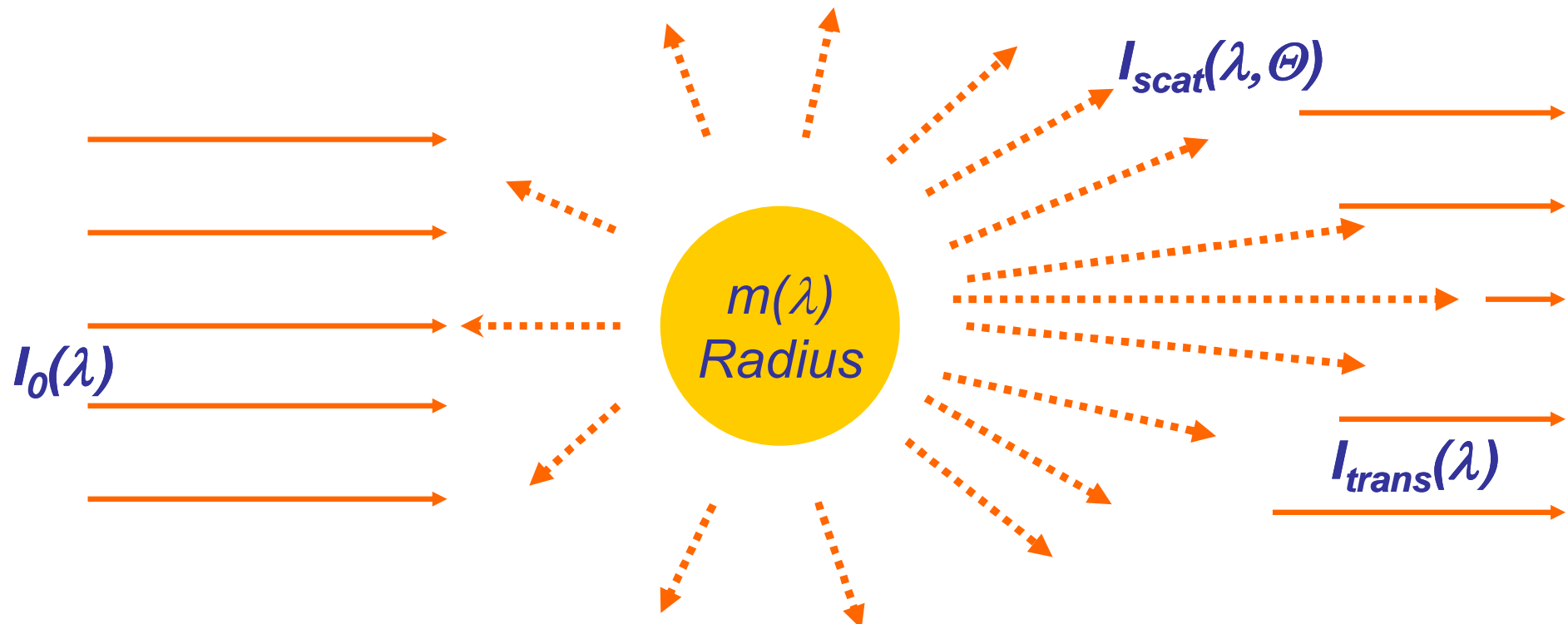
**BRDF, BPRF**

# Forward Model



# Single Scattering by Single Particle

**Scattering and Absorption** is modeled assuming aerosol particle as *homogeneous sphere* with **spectrally dependent complex refractive index** ( $m(\lambda) = n(\lambda) - i k(\lambda)$ ) - “Mie particles”



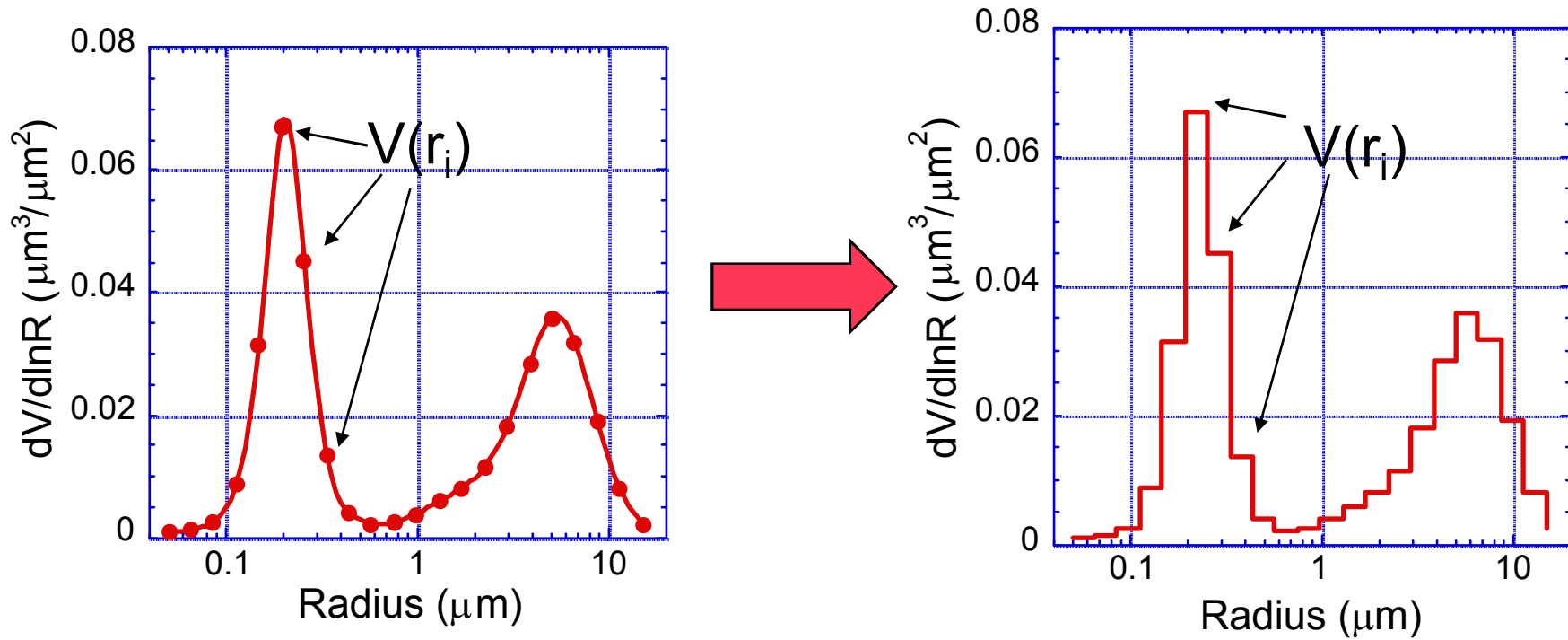
$P_{ii}(\Theta)$ - Phase Matrix;

$\tau(\lambda)$  - extinction optical thickness;

$\omega_0(\lambda)$  -single scattering albedo

$\tau(\lambda)\omega_0(\lambda)$  absorption optical thickness

# Modeling Polydispersions



$$\tau(\lambda) = \int_{r_{\min}}^{r_{\max}} K_\tau(\lambda; k; n; r) V(r) dr \approx \sum V(r_i) \int_{r_i - \Delta/2}^{r_i + \Delta/2} K_\tau(\lambda; k; n; r) dr$$

$K(\lambda; k; n; r_i)$

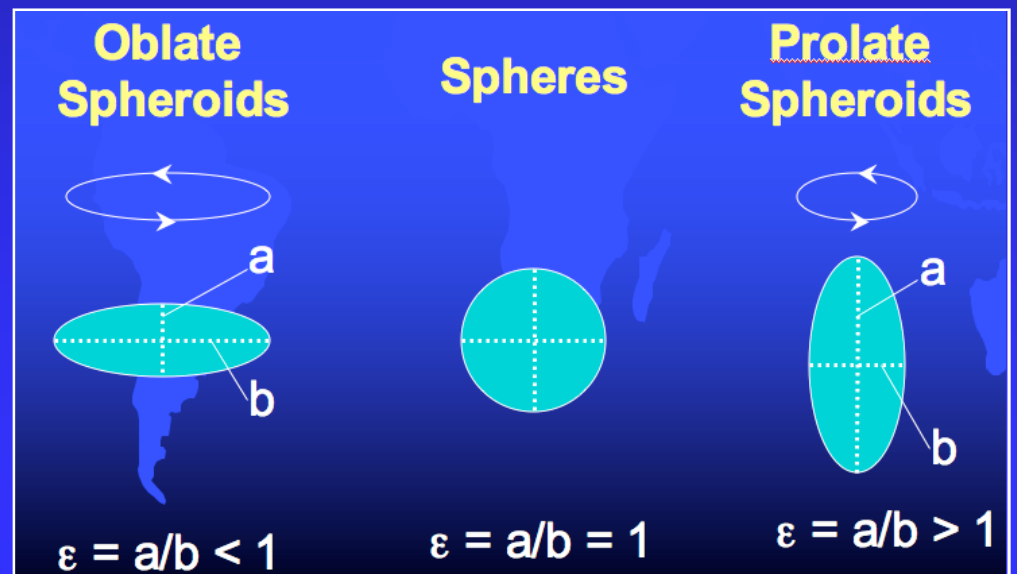
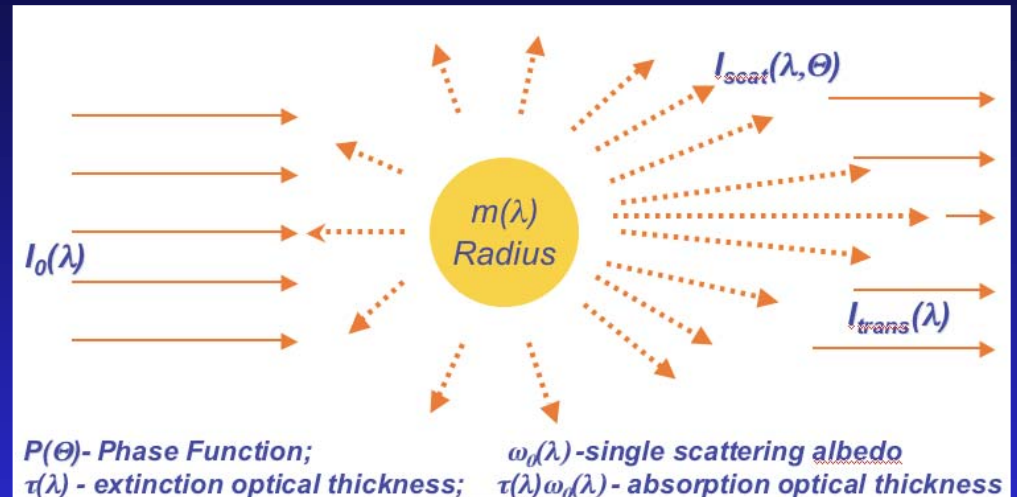
- Kernel look-up table for fixed  $r_i$  (22 points)  
 $(1.33 \leq n \leq 1.7; 0.0 \leq k \leq 0.5)$

# Aerosol single particle scattering:

**ASSUMPTIONS** in  
the retrievals:

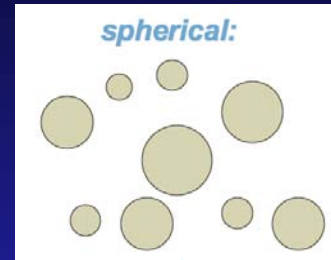
EACH AEROSOL PARTICLE

- sphere or spheroid (!!!);
- homogeneous;
- $1.33 \leq n \leq 1.7$
- $0.0 \leq k \leq 0.5$
- $n$  and  $k$  spectrally dependent  
*(but smooth)*

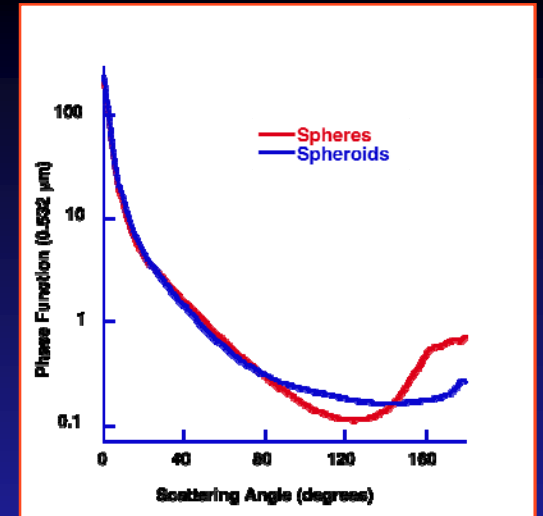


# Mixing of particle shapes retrieved

$C \times$



$+ (1-C) \times$



$$\tau(\lambda) = C \int_{r_{\min}}^{r_{\max}} K_{\tau}^{\text{spherical}}(k; n; r) V(r) dr + (1 - C) \int_{r_{\min}}^{r_{\max}} \left( \int_{\varepsilon_{\min}}^{\varepsilon_{\max}} K_{\tau}^{\varepsilon}(k; n; r, \varepsilon) N(\varepsilon) d\varepsilon \right) V(r) dr$$

Aspect ratio distr.

## ASSUMPTIONS:

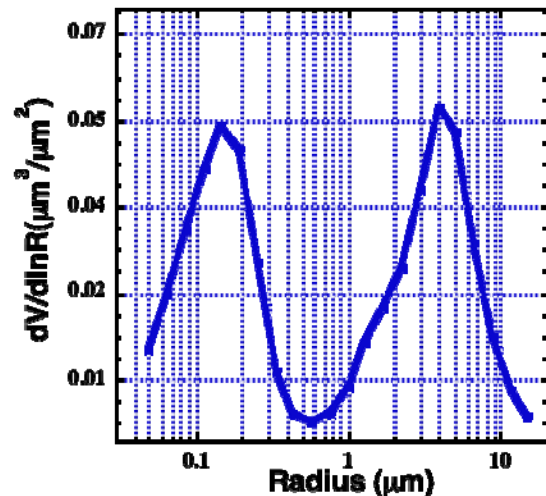
- $dV/dr$  - volume size distribution is the same for both components;
- non-spherical - mixture of randomly oriented polydisperse spheroids;
- aspect ratio distribution  $N(\varepsilon)$  is fixed to the retrieved by Dubovik et al. 2006

# Aerosol is driven by 31 variables in AERONET retrieval :

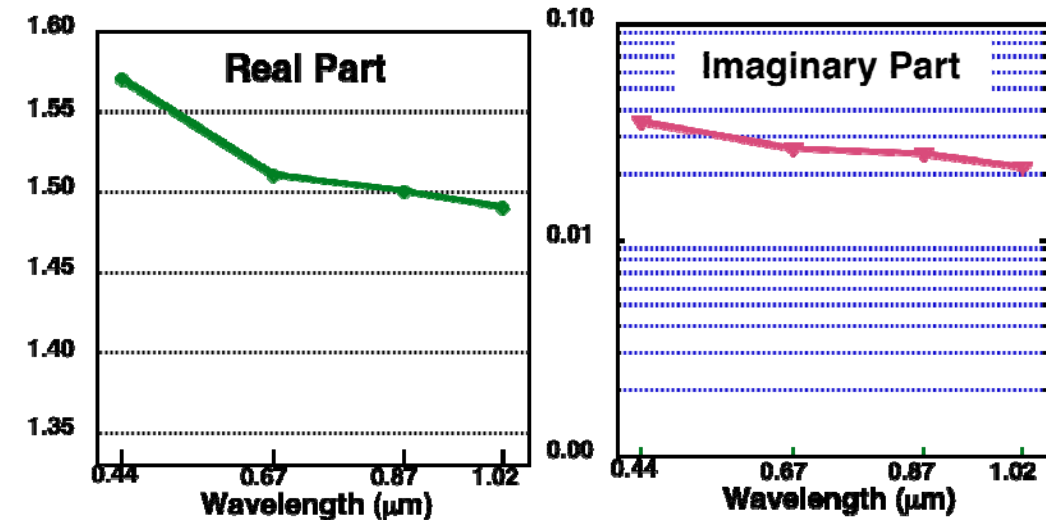
$dV/d\ln r$  - size distribution (~22 values);  
 $n(\lambda)$  and  $k(\lambda)$  - ref. index (4 +4 values)  
 $C_{\text{spher}} (\%)$  - spherical fraction (1 value)

Similar to AERONET model:

**Particle Size Distribution:**  
 $0.05 \mu\text{m} \leq R \text{ (22 bins)} \leq 15 \mu\text{m}$



**Complex Refractive Index at**  
 $\lambda = 0.44; 0.67; 0.87; 1.02 \mu\text{m}$



Smoke



Desert Dust



Maritime



# Inversion strategy

More details are given in paper:  
Dubovik and King [2000],  
"A flexible algorithm ..."

## ***Principles of statistical optimization:***

- all data (measured and a priori) are considered as **multi-source data** with **known** accuracy;
- the inversion is a search for the **best fit of all data** by forward model that **accounts** for the **accuracy levels** of the fitted data;

## ***Multi-source data include:***

1. **Measurements:**
  - spectral optical thickness;
  - angular distribution of sky-radiance;
2. ***A priori* smoothness constraints on**
  - particle size distribution;
  - spectral dependence of the real part of the index of refraction;
  - spectral dependence of the imaginary part of the index of refraction;

## Multi-sensor data

$$\left\{ \begin{array}{l} \text{sensor 1} \\ \text{sensor 2} \\ \dots \end{array} \right. \quad \left. \begin{array}{l} \mathbf{f}_1^* = \mathbf{F}_1 \mathbf{a} + \Delta_1 \\ \mathbf{f}_2^* = \mathbf{F}_2 \mathbf{a} + \Delta_2 \\ \dots \end{array} \right. \quad \text{Independent !!!}$$

## Multi-Term LSM

(e.g. see Dubovik and King 2000, Dubovik 2004)

$$\hat{\mathbf{a}} = \left( \mathbf{F}_1^T \mathbf{C}_1^{-1} \mathbf{F}_1 + \mathbf{F}_2^T \mathbf{C}_2^{-1} \mathbf{F}_2 + \dots \right)^{-1} \left( \mathbf{F}_1^T \mathbf{C}_1^{-1} \mathbf{f}_1^* + \mathbf{F}_2^T \mathbf{C}_2^{-1} \mathbf{f}_2^* + \dots \right)$$

## Single-sensor data

$$\left. \begin{array}{l} \text{sensor} \\ \text{a priori} \end{array} \right. \quad \left\{ \begin{array}{l} \mathbf{f}^* = \mathbf{F} \mathbf{a} + \Delta_f \\ \mathbf{a}^* = \mathbf{a} + \Delta_a \end{array} \right.$$

$$\hat{\mathbf{a}} = \left( \mathbf{F}^T \mathbf{C}_f^{-1} \mathbf{F} + \mathbf{C}_a^{-1} \right)^{-1} \left( \mathbf{F}^T \mathbf{C}_f^{-1} \mathbf{f}^* + \mathbf{C}_a^{-1} \mathbf{a}^* \right)$$

*“Optimum Estimations” by Rodgers  
Levenberg-Marquardt  
Maximum Entropy Method  
Kalman Filter ...,  
4D Variational Assimilation (4DVR)*

*...  
Phillips – Tikhonov - Twomey*

## Multi-sensor data

$$\begin{cases} \mathbf{f}_1^* = \mathbf{F}_1 \mathbf{a} + \Delta_1 \\ \mathbf{f}_2^* = \mathbf{F}_2 \mathbf{a} + \Delta_2 \\ \dots \end{cases}$$

*sensor 1*  
*sensor 2*      *Independent !!!*

## Multi-Term LSM

(e.g. see Dubovik 2004)

$$\hat{\mathbf{a}} = \left( \mathbf{F}_1^T \mathbf{C}_1^{-1} \mathbf{F}_1 + \mathbf{F}_2^T \mathbf{C}_2^{-1} \mathbf{F}_2 + \dots \right)^{-1} \left( \mathbf{F}_1^T \mathbf{C}_1^{-1} \mathbf{f}_1^* + \mathbf{F}_2^T \mathbf{C}_2^{-1} \mathbf{f}_2^* + \dots \right)$$

## Single-sensor data

*sensor*  
*a priori*

$$\begin{cases} \mathbf{f}_1^\bullet = \mathbf{f}^* = \mathbf{F} \mathbf{a} + \Delta_f \\ \mathbf{f}_2^\bullet = \mathbf{0}^* = \mathbf{S} \mathbf{a} + \Delta(\Delta \mathbf{a}) \end{cases}$$

$$\hat{\mathbf{a}} = \left( \mathbf{F}^T \mathbf{C}_f^{-1} \mathbf{F} + \mathbf{S}^T \mathbf{S} \right)^{-1} \left( \mathbf{F}^T \mathbf{C}_f^{-1} \mathbf{f}^* \right)$$

*Phillips-Tikhonov-Twomey formula*

## A priori restrictions on smoothness

A priori equation system

Normally distributed errors  
with variance  $\varepsilon_i^2$

$$\theta^* = (\Delta \mathbf{a})^* = \mathbf{S} \mathbf{a} + \Delta(\Delta \mathbf{a})$$

$$\frac{\partial V(a)}{\partial a} =$$

Coefficients of differences/derivatives:

e.g. for second dif. ( $k=2$ ),

$$\begin{aligned}\Delta^2 &= (\hat{a}_{i+2} - \hat{a}_{i+1}) - (\hat{a}_{i+1} - \hat{a}_i) \\ &= \hat{a}_{i+2} - 2\hat{a}_{i+1} + \hat{a}_i:\end{aligned}$$

$$\mathbf{S}_2 = \begin{pmatrix} 1 & -2 & 1 & 0 & \dots \\ 0 & 1 & -2 & 1 & 0 & \dots \\ 0 & 0 & 1 & -2 & 1 & 0 & \dots \\ \dots & \dots & \dots & \dots & \dots & \dots \\ \dots & \dots & \dots & \dots & 0 & 1 & -2 & 1 \end{pmatrix}$$

# Statistically Optimized Minimization - Fitting

POLDER/PARASOL

$$\hat{\mathbf{a}} = \left( \mathbf{F}_1^T \mathbf{C}_1^{-1} \mathbf{F}_1 + \mathbf{F}_2^T \mathbf{C}_2^{-1} \mathbf{F}_2 + \dots \right)^{-1} \left( \mathbf{F}_1^T \mathbf{C}_1^{-1} \mathbf{f}_1^* + \mathbf{F}_2^T \mathbf{C}_2^{-1} \mathbf{f}_2^* + \dots \right)$$

## Measurements:

-their covariances

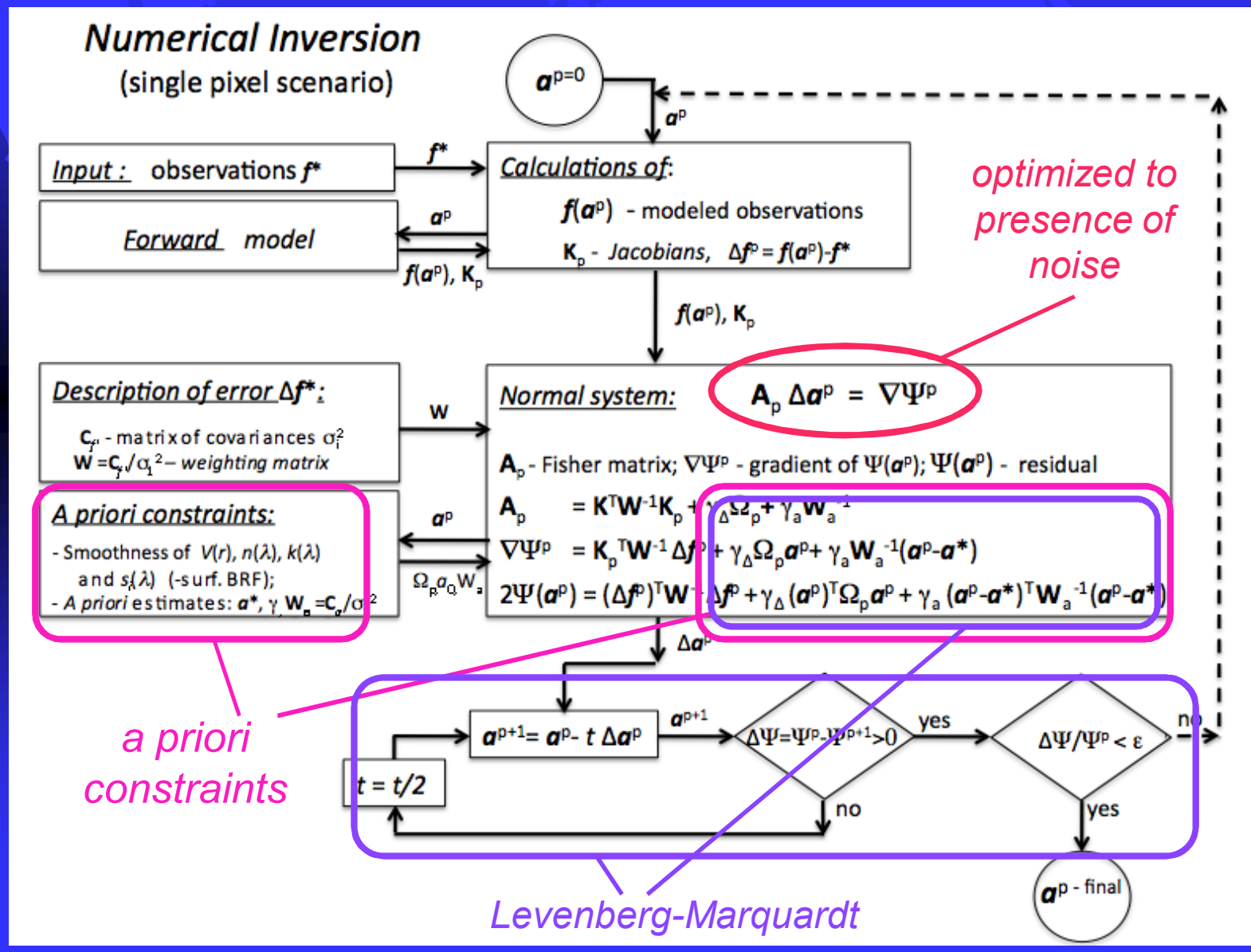
(should depend on  $\lambda$  and  $\Theta$ )

-lognormal error  
distributions

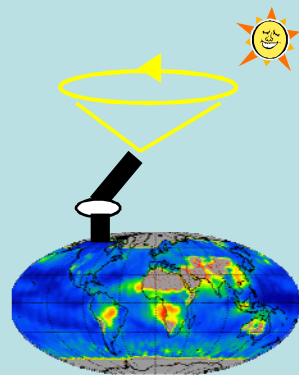
*a priori* restrictions on  
norms of derivatives of:  
 $i=2$  -size distr. variability;  
 $i=3$  -n spectral variability;  
 $i=4$  -k spectral variability;

# « AERONET like » statistically optimized « no look-up tables » inversion

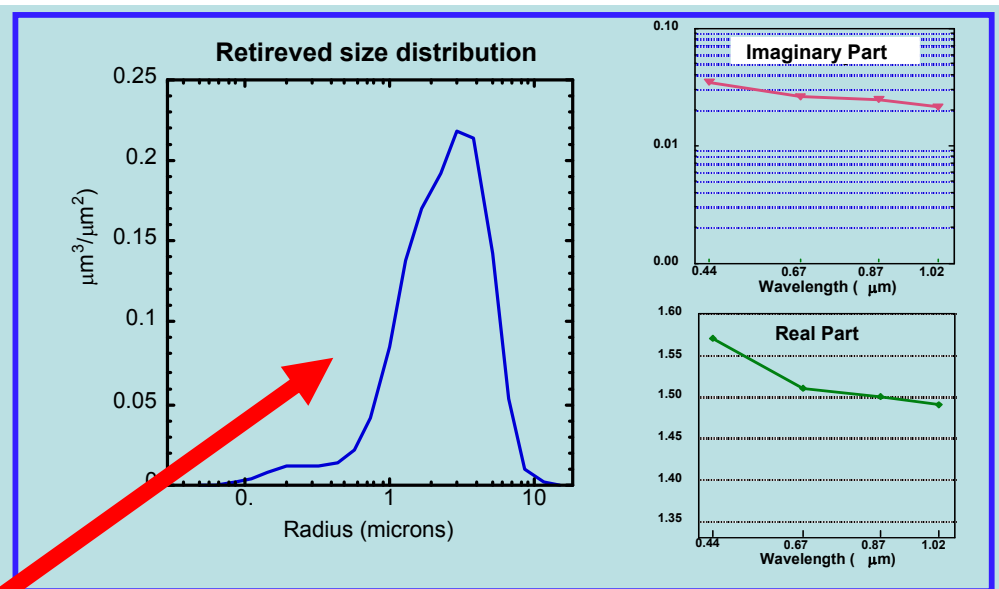
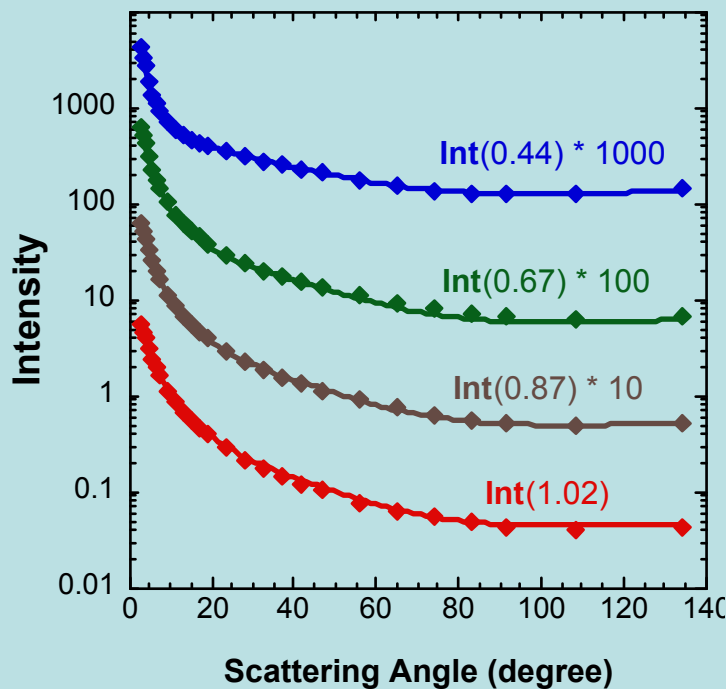
Dubovik et al., AMT, 2011



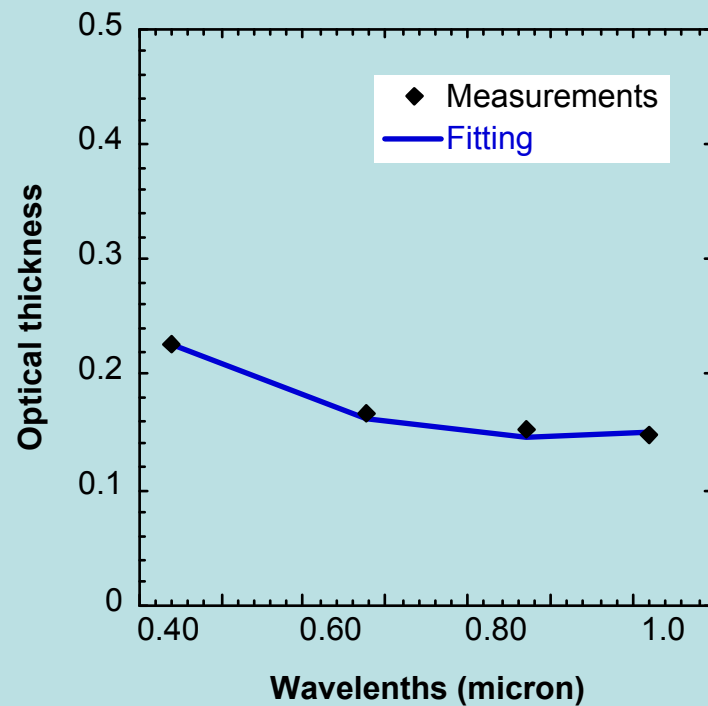
# Fitting as a retrieval strategy



Almucantar Fitting

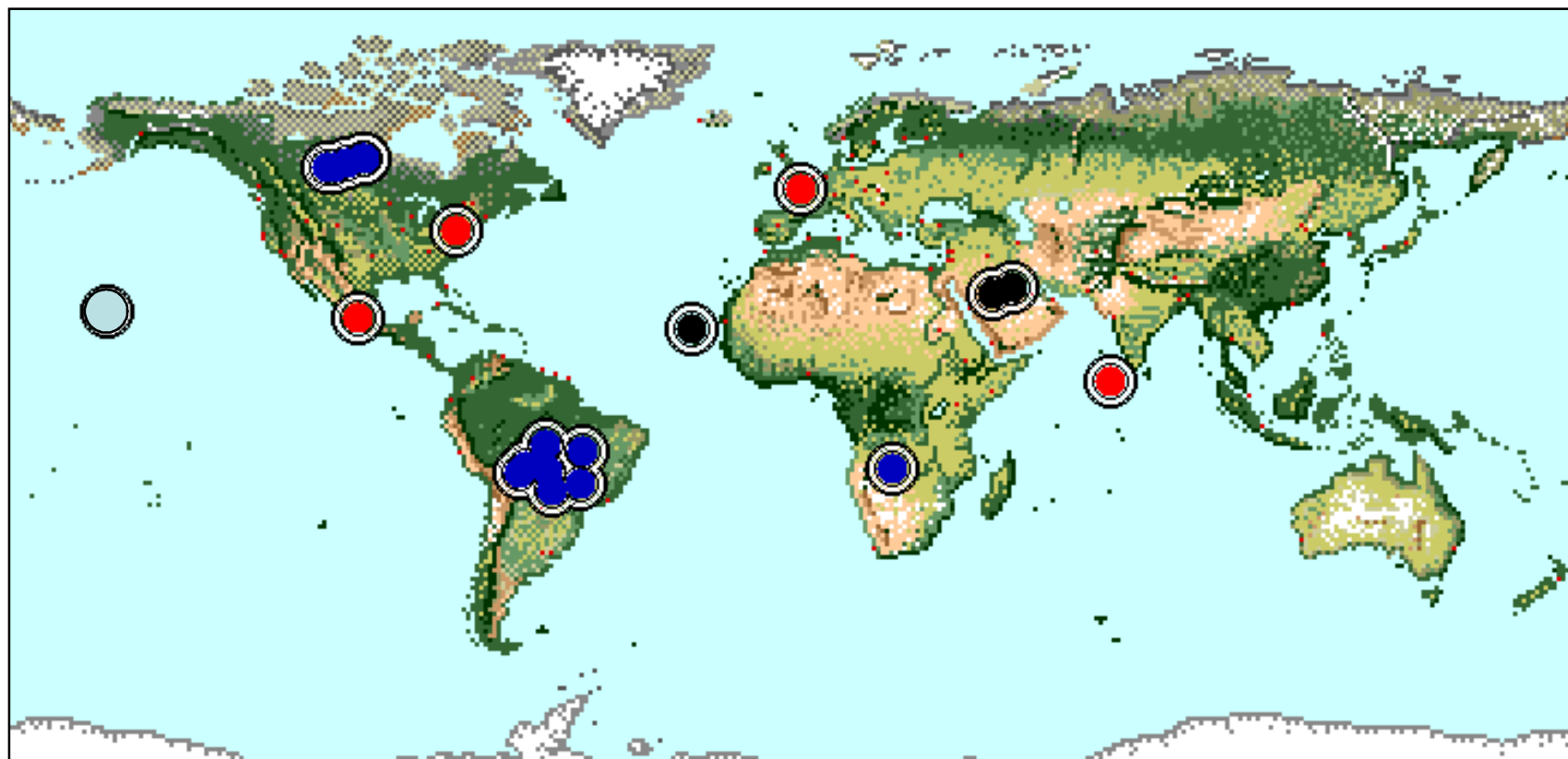


Fitting of optical thickness in retrievals



# Observation Sites for Climatology

- - Urban/Industrial (*GSFC, Paris, Mexico-City, INDOEX*)
- - Biomass Burning (*Savanna, Cerrado, Forest*)
- - Desert Dust (*Cape Verde, Saudi Arabia, Persian Gulf*)
- - Oceanic Aerosol (*Hawaii*)



# The averaged optical properties of various aerosol types (Dubovik et al., 2002, JAS)

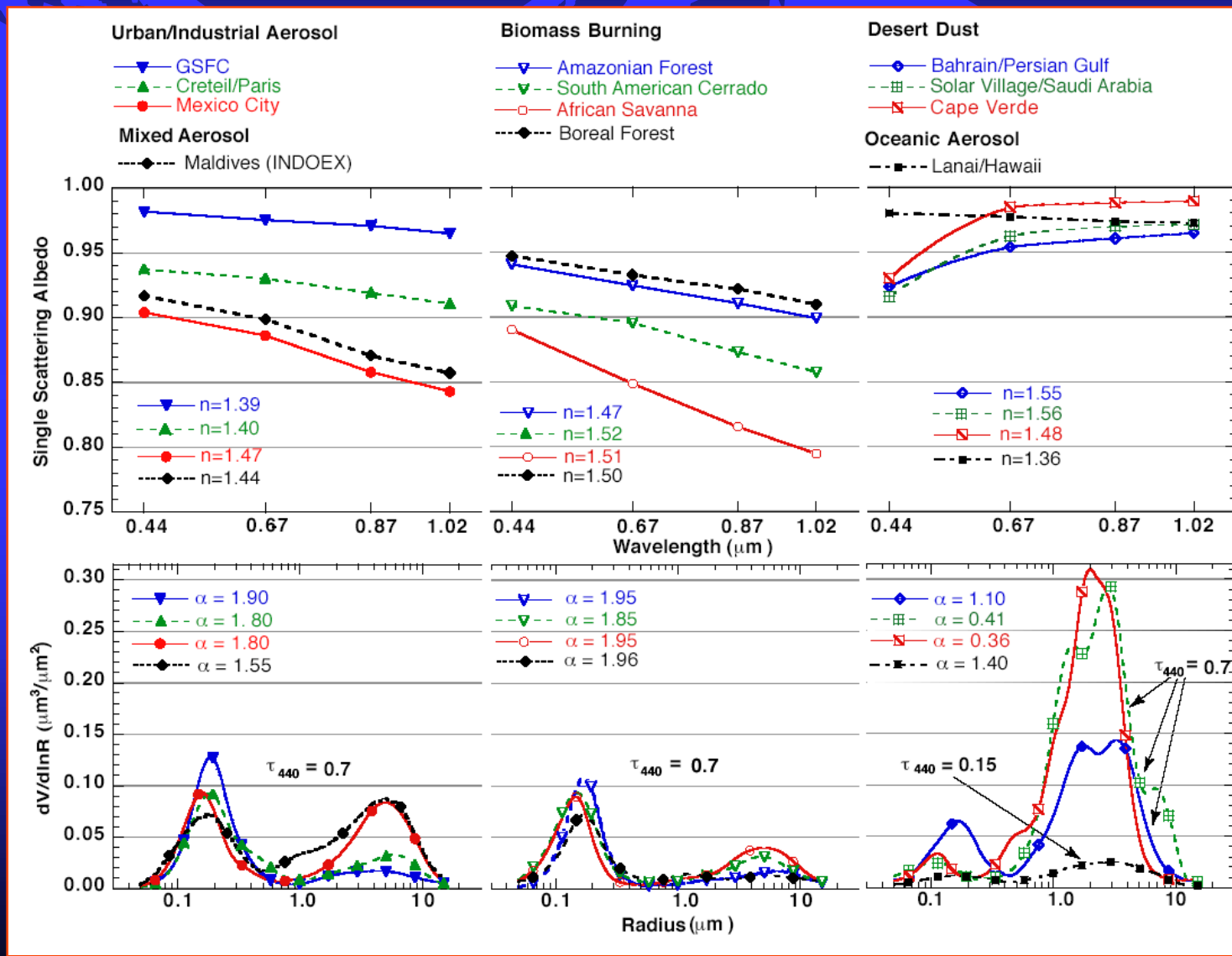


**Table 1.** Summary of aerosol optical properties retrieved from worldwide AERONET network of ground-based radiometers.

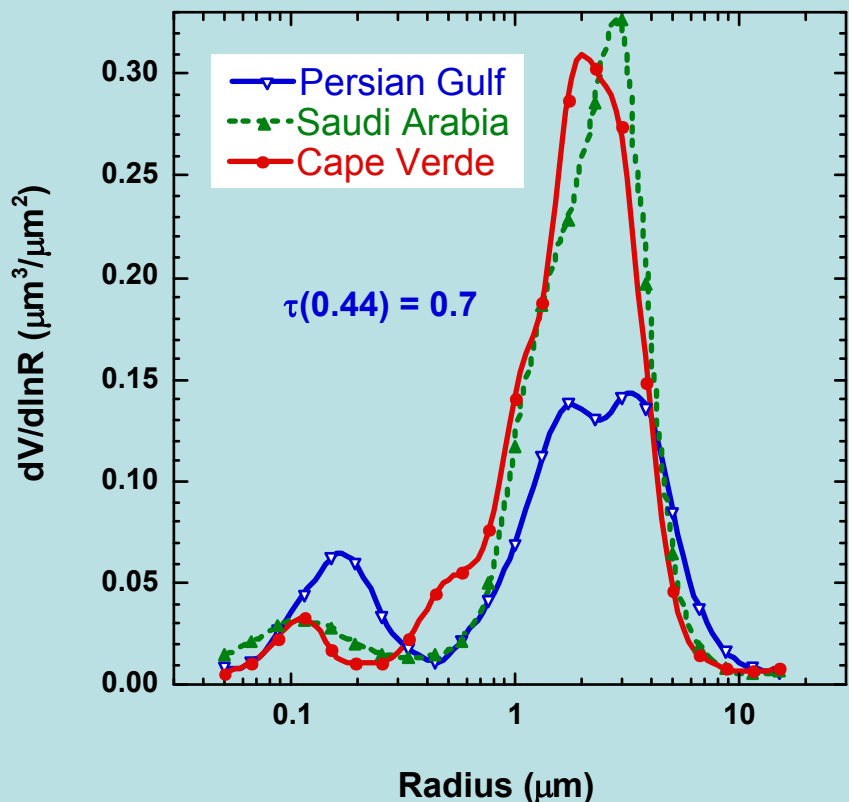
| <b>Urban/Industrial &amp; Mixed:</b>               | <b>GSFC/ Greenbelt /USA (1993-2000)</b>                           | <b>Creteil/ Paris France (1999)</b>                               | <b>Mexico City (1999 - 2000)</b>                                  | <b>Maldives (INDOEX) (1999-2000)</b>                               |
|----------------------------------------------------|-------------------------------------------------------------------|-------------------------------------------------------------------|-------------------------------------------------------------------|--------------------------------------------------------------------|
| Number of meas. (total)                            | 2400                                                              | 300                                                               | 1500                                                              | 700                                                                |
| Number of meas. (for $\omega_0, n, k$ )            | 200 (June - September)                                            | 40 (June - September)                                             | 300                                                               | 150 (January - April)                                              |
| Range of optical thickness; $\langle \tau \rangle$ | $0.1 \leq \tau(440) \leq 1.0; \langle \tau(440) \rangle = 0.24$   | $0.1 \leq \tau(440) \leq 0.9; \langle \tau(440) \rangle = 0.26$   | $0.1 \leq \tau(440) \leq 1.8; \langle \tau(440) \rangle = 0.43$   | $0.1 \leq \tau(440) \leq 0.7; \langle \tau(440) \rangle = 0.27$    |
| Range of $\epsilon$ ngstrom parameter              | $1.2 \leq \alpha \leq 2.5$                                        | $1.2 \leq \alpha \leq 2.3$                                        | $1.0 \leq \alpha \leq 2.3$                                        | $0.4 \leq \alpha \leq 2.0$                                         |
| $\langle g \rangle (440/ 670/ 870/ 1020)$          | $0.68/ 0.59/ 0.54/ 0.53 \pm 0.08$                                 |                                                                   |                                                                   |                                                                    |
| $n; k$                                             | $1.41 - 0.03\tau(440) \pm 0.01; 0.003 \pm 0.003$                  | $1.40 \pm 0.03; 0.009 \pm 0.004$                                  | $1.47 \pm 0.03; 0.014 \pm 0.006$                                  | $1.44 \pm 0.02; 0.011 \pm 0.007$                                   |
| $\omega_0(440/ 670/ 870/ 1020)$                    | $0.98/ 0.97/ 0.96/ 0.95 \pm 0.02$                                 | $0.94/ 0.93/ 0.92/ 0.91 \pm 0.03$                                 | $0.90/ 0.88/ 0.85/ 0.83 \pm 0.02$                                 | $0.91/ 0.89/ 0.86/ 0.84 \pm 0.03$                                  |
| $r_{vf}$ ( $\mu\text{m}$ ); $\sigma_r$             | $0.12 + 0.11\tau(440) \pm 0.03; 0.38 \pm 0.01$                    | $0.11 + 0.13\tau(440) \pm 0.03; 0.43 \pm 0.05$                    | $0.12 + 0.04\tau(440) \pm 0.02; 0.43 \pm 0.03$                    | $0.18 \pm 0.03; 0.46 \pm 0.04$                                     |
| $r_{vc}$ ( $\mu\text{m}$ ); $\sigma_c$             | $3.03 + 0.49\tau(440) \pm 0.21; 0.75 \pm 0.03$                    | $2.76 + 0.48\tau(440) \pm 0.30; 0.79 \pm 0.05$                    | $2.72 + 0.60\tau(440) \pm 0.23; 0.63 \pm 0.05$                    | $2.62 + 0.61\tau(440) \pm 0.31; 0.76 \pm 0.05$                     |
| $C_{vf}(\mu\text{m}^3/\mu\text{m}^2)$              | $0.15\tau(440) \pm 0.03$                                          | $0.01 + 0.12\tau(440) \pm 0.04$                                   | $0.12\tau(440) \pm 0.03$                                          | $0.12\tau(440) \pm 0.03$                                           |
| $C_{vc}(\mu\text{m}^3/\mu\text{m}^2)$              | $0.01 + 0.04\tau(440) \pm 0.01$                                   | $0.01 + 0.05\tau(440) \pm 0.02$                                   | $0.11\tau(440) \pm 0.03$                                          | $0.15\tau(440) \pm 0.04$                                           |
| <b>Biomass burning:</b>                            | <b>Amazonian Forest: Brazil (1993-1994); Bolivia (1998-1999);</b> | <b>South American Cerrado: Brazil (1993-1995)</b>                 | <b>African Savanna: Zambia (1995 - 2000)</b>                      | <b>Boreal Forest: USA, Canada (1994 - 1998)</b>                    |
| Number of meas. (total)                            | 700                                                               | 550                                                               | 2000                                                              | 1000                                                               |
| Number of meas. (for $\omega_0, n, k$ )            | 250 (August - October)                                            | 350 (August - October)                                            | 700 (August - November)                                           | 250 (June - September)                                             |
| Range of optical thickness; $\langle \tau \rangle$ | $0.1 \leq \tau(440) \leq 3.0; \langle \tau(440) \rangle = 0.74$   | $0.1 \leq \tau(440) \leq 2.1; \langle \tau(440) \rangle = 0.80$   | $0.1 \leq \tau(440) \leq 1.5; \langle \tau(440) \rangle = 0.38$   | $0.1 \leq \tau(440) \leq 2.0; \langle \tau(440) \rangle = 0.40$    |
| Range of $\epsilon$ ngstrom parameter              | $1.2 \leq \alpha \leq 2.1$                                        | $1.2 \leq \alpha \leq 2.1$                                        | $1.4 \leq \alpha \leq 2.2$                                        | $1.0 \leq \alpha \leq 2.3$                                         |
| $\langle g \rangle (440/ 670/ 870/ 1020)$          | $0.69/ 0.58/ 0.51/ 0.48 \pm 0.06$                                 | $0.67/ 0.59/ 0.55/ 0.53 \pm 0.03$                                 | $0.64/ 0.53/ 0.48/ 0.47 \pm 0.06$                                 | $0.69/ 0.61/ 0.55/ 0.53 \pm 0.06$                                  |
| $n; k$                                             | $1.47 \pm 0.03; 0.0093 \pm 0.003$                                 | $1.52 \pm 0.01; 0.015 \pm 0.004$                                  | $1.51 \pm 0.01; 0.021 \pm 0.004$                                  | $1.50 \pm 0.04; 0.0094 \pm 0.003$                                  |
| $\omega_0(440/ 670/ 870/ 1020)$                    | $0.94/ 0.93/ 0.91/ 0.90 \pm 0.02$                                 | $0.91/ 0.89/ 0.87/ 0.85 \pm 0.03$                                 | $0.88/ 0.84/ 0.80/ 0.78 \pm 0.015$                                | $0.94/ 0.935/ 0.92/ 0.91 \pm 0.02$                                 |
| $r_{vf}$ ( $\mu\text{m}$ ); $\sigma_r$             | $0.14 + 0.013\tau(440) \pm 0.01; 0.40 \pm 0.04$                   | $0.14 + 0.01\tau(440) \pm 0.01; 0.47 \pm 0.03$                    | $0.12 + 0.025\tau(440) \pm 0.01; 0.40 \pm 0.01$                   | $0.15 + 0.015\tau(440) \pm 0.01; 0.43 \pm 0.01$                    |
| $r_{vc}$ ( $\mu\text{m}$ ); $\sigma_c$             | $3.27 + 0.58\tau(440) \pm 0.45; 0.79 \pm 0.06$                    | $3.27 + 0.51\tau(440) \pm 0.39; 0.79 \pm 0.04$                    | $3.22 + 0.71\tau(440) \pm 0.43; 0.73 \pm 0.03$                    | $3.21 + 0.2\tau(440) \pm 0.23; 0.81 \pm 0.2$                       |
| $C_{vf}(\mu\text{m}^3/\mu\text{m}^2)$              | $0.12\tau(440) \pm 0.05$                                          | $0.1\tau(440) \pm 0.06$                                           | $0.12\tau(440) \pm 0.04$                                          | $0.01 + 0.1\tau(440) \pm 0.04$                                     |
| $C_{vc}(\mu\text{m}^3/\mu\text{m}^2)$              | $0.05\tau(440) \pm 0.02$                                          | $0.04 + 0.03\tau(440) \pm 0.03$                                   | $0.09\tau(440) \pm 0.02$                                          | $0.01 + 0.03\tau(440) \pm 0.03$                                    |
| <b>Desert Dust &amp; Oceanic:</b>                  | <b>Bahrain/ Persian Gulf (1998 - 2000)</b>                        | <b>Solar-Vil/ Saudi Arabia (1998-2000)</b>                        | <b>Cape Verde (1993 - 2000)</b>                                   | <b>Lanai/Hawaii (1995-2000)</b>                                    |
| Number of meas. (total)                            | 1800                                                              | 1500                                                              | 1500                                                              | 800                                                                |
| Number of meas. (for $\omega_0, n, k$ )            | 100                                                               | 250                                                               | 300                                                               | 150                                                                |
| Range of optical thickness; $\langle \tau \rangle$ | $0.1 \leq \tau(1020) \leq 1.2, \langle \tau(1020) \rangle = 0.22$ | $0.1 \leq \tau(1020) \leq 1.5; \langle \tau(1020) \rangle = 0.17$ | $0.1 \leq \tau(1020) \leq 2.0; \langle \tau(1020) \rangle = 0.39$ | $0.01 \leq \tau(1020) \leq 0.2; \langle \tau(1020) \rangle = 0.04$ |
| Range of $\epsilon$ ngstrom parameter              | $0 \leq \alpha \leq 1.6$                                          | $0.1 \leq \alpha \leq 0.9$                                        | $-0.1 \leq \alpha \leq 0.7$                                       | $0 \leq \alpha \leq 1.55$                                          |
| $\langle g \rangle (440/ 670/ 870/ 1020)$          | $0.68/ 0.66/ 0.66/ 0.66 \pm 0.04$                                 | $0.69/ 0.66/ 0.65/ 0.65 \pm 0.04$                                 | $0.73/ 0.71/ 0.71/ 0.71 \pm 0.04$                                 | $0.75/ 0.71/ 0.69/ 0.68 \pm 0.04$                                  |
| $n$                                                | $1.55 \pm 0.03$                                                   | $1.56 \pm 0.03$                                                   | $1.48 \pm 0.05$                                                   | $1.36 \pm 0.01$                                                    |
| $k(440/ 670/ 870/ 1020)$                           | $0.0025/ 0.0014/ 0.001/ 0.001 \pm 0.001$                          | $0.0029/ 0.0013/ 0.001/ 0.001 \pm 0.001$                          | $0.0025/ 0.0007/ 0.0006/ 0.0006 \pm 0.001$                        | $0.0015 \pm 0.001$                                                 |
| $\omega_0(440/ 670/ 870/ 1020)$                    | $0.92/ 0.95/ 0.96/ 0.97 \pm 0.03$                                 | $0.92/ 0.96/ 0.97/ 0.97 \pm 0.02$                                 | $0.93/ 0.98/ 0.99/ 0.99 \pm 0.01$                                 | $0.98/ 0.97/ 0.97/ 0.97 \pm 0.03$                                  |
| $r_{vf}$ ( $\mu\text{m}$ ); $\sigma_r$             | $0.15 \pm 0.04; 0.42 \pm 0.04$                                    | $0.12 \pm 0.05; 0.40 \pm 0.05$                                    | $0.12 \pm 0.03; 0.49 + 0.10\tau \pm 0.04$                         | $0.16 \pm 0.02; 0.48 \pm 0.04$                                     |
| $r_{vc}$ ( $\mu\text{m}$ ); $\sigma_c$             | $2.54 \pm 0.04; 0.61 \pm 0.02$                                    | $2.32 \pm 0.03; 0.60 \pm 0.03$                                    | $1.90 \pm 0.03; 0.63 - 0.10\tau \pm 0.03$                         | $2.70 \pm 0.04; 0.68 \pm 0.04$                                     |
| $C_{vf}(\mu\text{m}^3/\mu\text{m}^2)$              | $0.02 + 0.1\tau(1020) \pm 0.05$                                   | $0.02 + 0.02\tau(1020) \pm 0.03$                                  | $0.02 + 0.02\tau(1020) \pm 0.03$                                  | $0.40\tau(1020) \pm 0.01$                                          |
| $C_{vc}(\mu\text{m}^3/\mu\text{m}^2)$              | $-0.02 + 0.92\tau(1020) \pm 0.04$                                 | $-0.02 + 0.98\tau(1020) \pm 0.04$                                 | $0.9\tau(1020) \pm 0.09$                                          | $0.80\tau(1020) \pm 0.02$                                          |

# Retrieved Properties of Saharan Dust

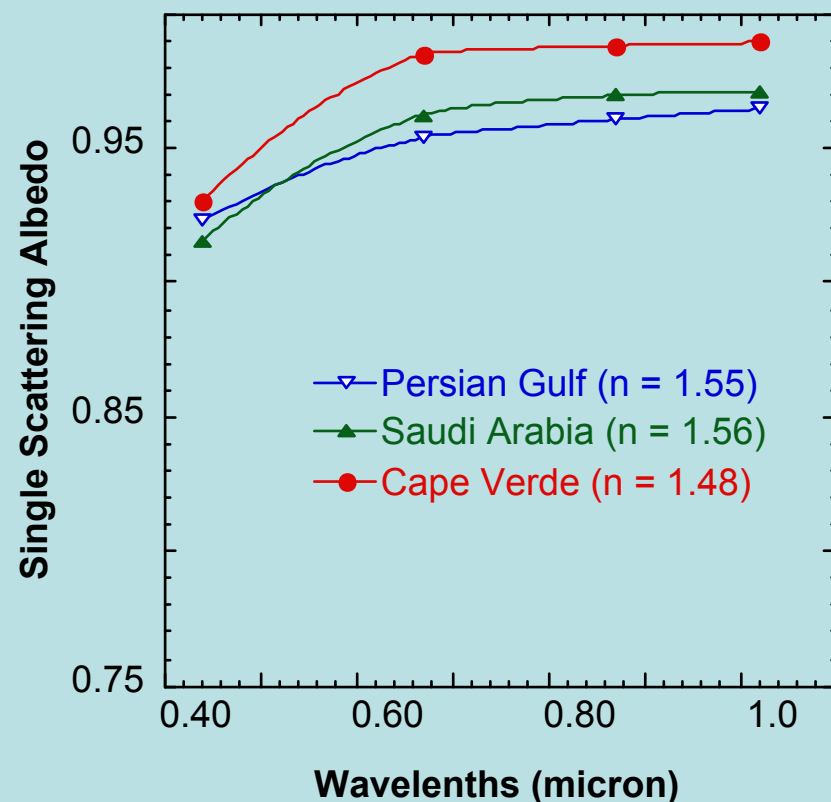
Angstrom < 0.75

Dubovik et al., 2002

Average Size Distributions

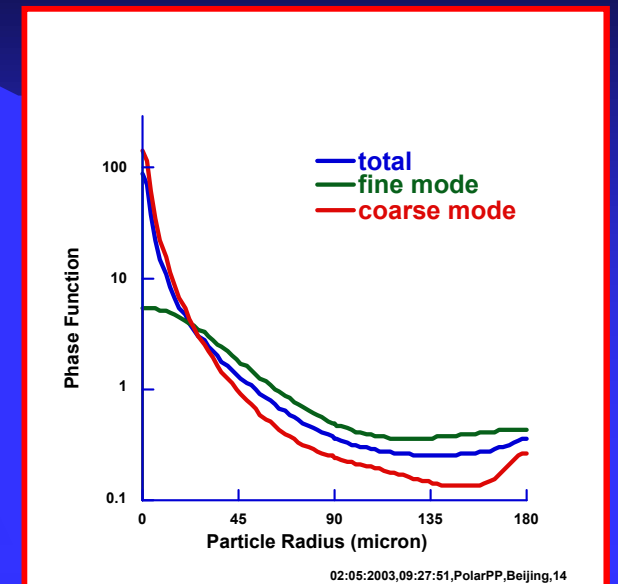
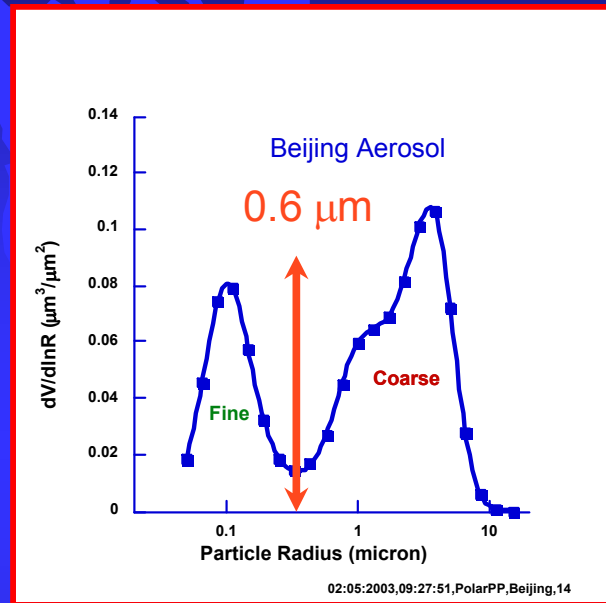


Average Single Scattering Albedo



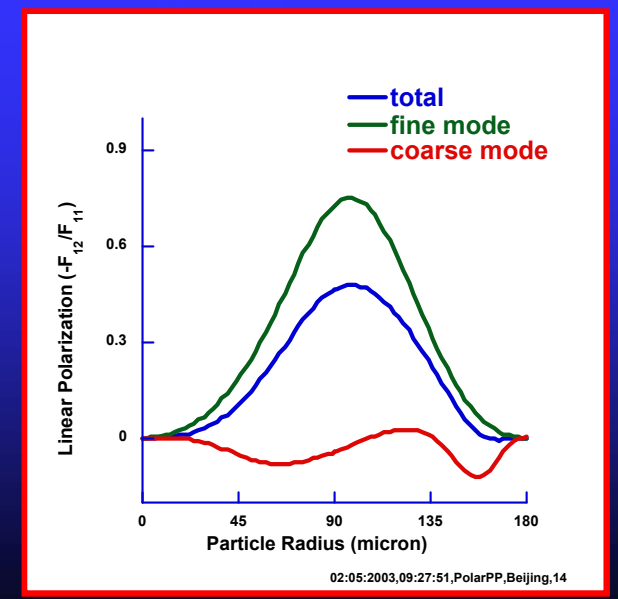
# Fine / Coarse modes parameters:

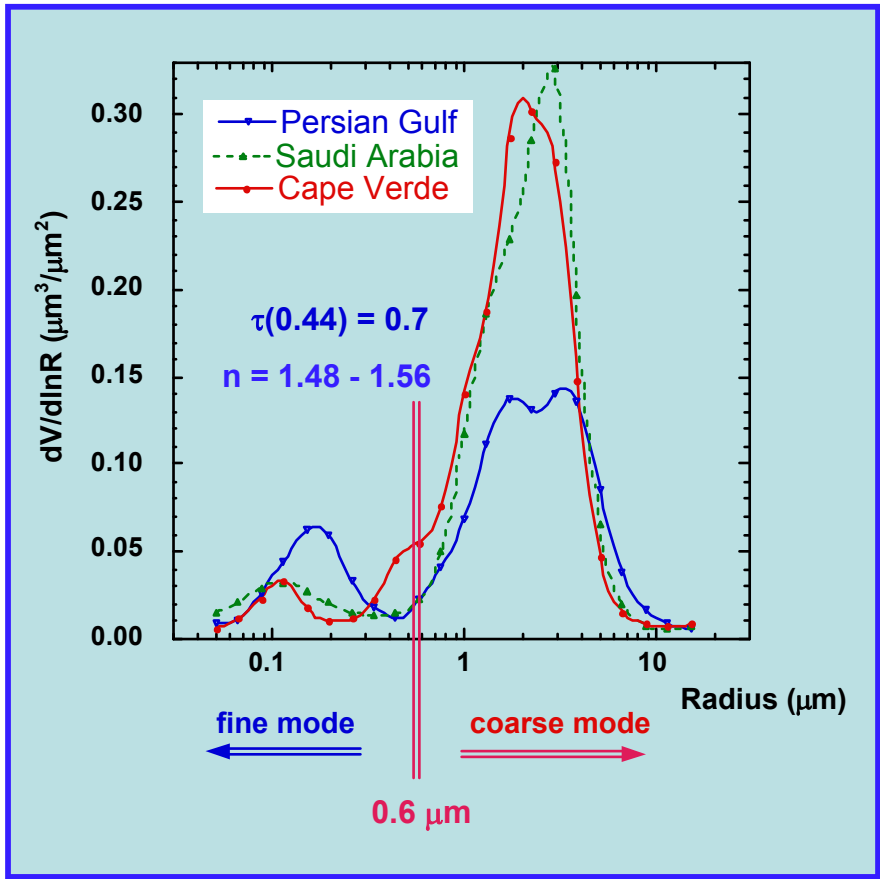
Flexible separation:  
minimum between: 0.194 and 0.576  $\mu\text{m}$



Integral parameters of  $dV/d\ln R$ :

t - total; f - fine ; c - coarse  
C(t,f,c) - Volume Concentration  
 $R_v(t,f,c)$  - Mean Radius  
 $\sigma(t,f,c)$  - Standard Deviation  
 $R_{\text{eff}}(t,f,c)$  - Effective Radius



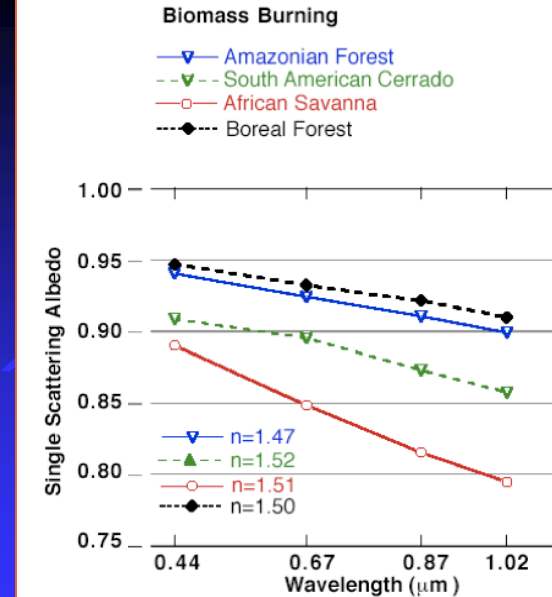


## Parameters of Bi-Modal Size Distributions:

|                                     |                                |
|-------------------------------------|--------------------------------|
| $V_{\text{coarse}}/V_{\text{fine}}$ | $\sim 10 \text{ (15 - 5)}$     |
| $R_{\text{coarse}}$                 | $\sim 2.6 - 1.9 \mu\text{m}$   |
| $R_{\text{fine}}$                   | $\sim 0.12 - 0.16 \mu\text{m}$ |
| $\sigma_{\text{coarse}}$            | $\sim 0.60$                    |
| $\sigma_{\text{fine}}$              | $\sim 0.40$                    |

Table from *Dubovik et al., 2002*

| Desert Dust                                                                        | Bahrain/ Persian Gulf (1998 - 2000)                               | Solar-Vil./ Saudi Arabia (1998-2000)                              | Cape Verde (1993 - 2000)                                          |
|------------------------------------------------------------------------------------|-------------------------------------------------------------------|-------------------------------------------------------------------|-------------------------------------------------------------------|
| Number of meas. (total)                                                            | 1800                                                              | 1500                                                              | 1500                                                              |
| Number of meas. (for $\omega_0, n, k$ )                                            | 100                                                               | 250                                                               | 300                                                               |
| Range of optical thickness; $\langle \tau \rangle$                                 | $0.1 \leq \tau(1020) \leq 1.2, \langle \tau(1020) \rangle = 0.22$ | $0.1 \leq \tau(1020) \leq 1.5; \langle \tau(1020) \rangle = 0.17$ | $0.1 \leq \tau(1020) \leq 2.0; \langle \tau(1020) \rangle = 0.39$ |
| Range of $\epsilon$ ngstrom parameter<br>$\langle g \rangle$ (440/ 670/ 870/ 1020) | $0 \leq \alpha \leq 1.6$<br>$0.68/ 0.66/ 0.66/ 0.66 \pm 0.04$     | $0.1 \leq \alpha \leq 0.9$<br>$0.69/ 0.66/ 0.65/ 0.65 \pm 0.04$   | $-0.1 \leq \alpha \leq 0.7$<br>$0.73/ 0.71/ 0.71/ 0.71 \pm 0.04$  |
| $n$                                                                                | $1.55 \pm 0.03$                                                   | $1.56 \pm 0.03$                                                   | $1.48 \pm 0.05$                                                   |
| $k(440/ 670/ 870/ 1020)$                                                           | $0.0025/ 0.0014 / 0.001 / 0.001 \pm 0.001$                        | $0.0029 / 0.0013 / 0.001 / 0.001 \pm 0.001$                       | $0.0025 / 0.0007 / 0.0006 / 0.0006 \pm 0.001$                     |
| $\omega_0(440/ 670/ 870/ 1020)$                                                    | $0.92 / 0.95 / 0.96 / 0.97 \pm 0.03$                              | $0.92 / 0.96 / 0.97 / 0.97 \pm 0.02$                              | $0.93 / 0.98 / 0.99 / 0.99 \pm 0.01$                              |
| $r_{vf} (\mu\text{m}); \sigma_f$                                                   | $0.15 \pm 0.04; 0.42 \pm 0.04$                                    | $0.12 \pm 0.05; 0.40 \pm 0.05$                                    | $0.12 \pm 0.03; 0.49 + 0.10 \tau \pm 0.04$                        |
| $r_{vc} (\mu\text{m}); \sigma_c$                                                   | $2.54 \pm 0.04; 0.61 \pm 0.02$                                    | $2.32 \pm 0.03; 0.60 \pm 0.03$                                    | $1.90 \pm 0.03; 0.63 - 0.10 \tau \pm 0.03$                        |
| $C_{vf} (\mu\text{m}^3/\mu\text{m}^2)$                                             | $0.02 + 0.1 \tau(1020) \pm 0.05$                                  | $0.02 + 0.02 \tau(1020) \pm 0.03$                                 | $0.02 + 0.02 \tau(1020) \pm 0.03$                                 |
| $C_{vc} (\mu\text{m}^3/\mu\text{m}^2)$                                             | $-0.02 + 0.92 \tau(1020) \pm 0.04$                                | $-0.02 + 0.98 \tau(1020) \pm 0.04$                                | $0.9 \tau(1020) \pm 0.09$                                         |



# ABSORPTION of SMOKE

flaming combustion  
Rio Branco, Brazil

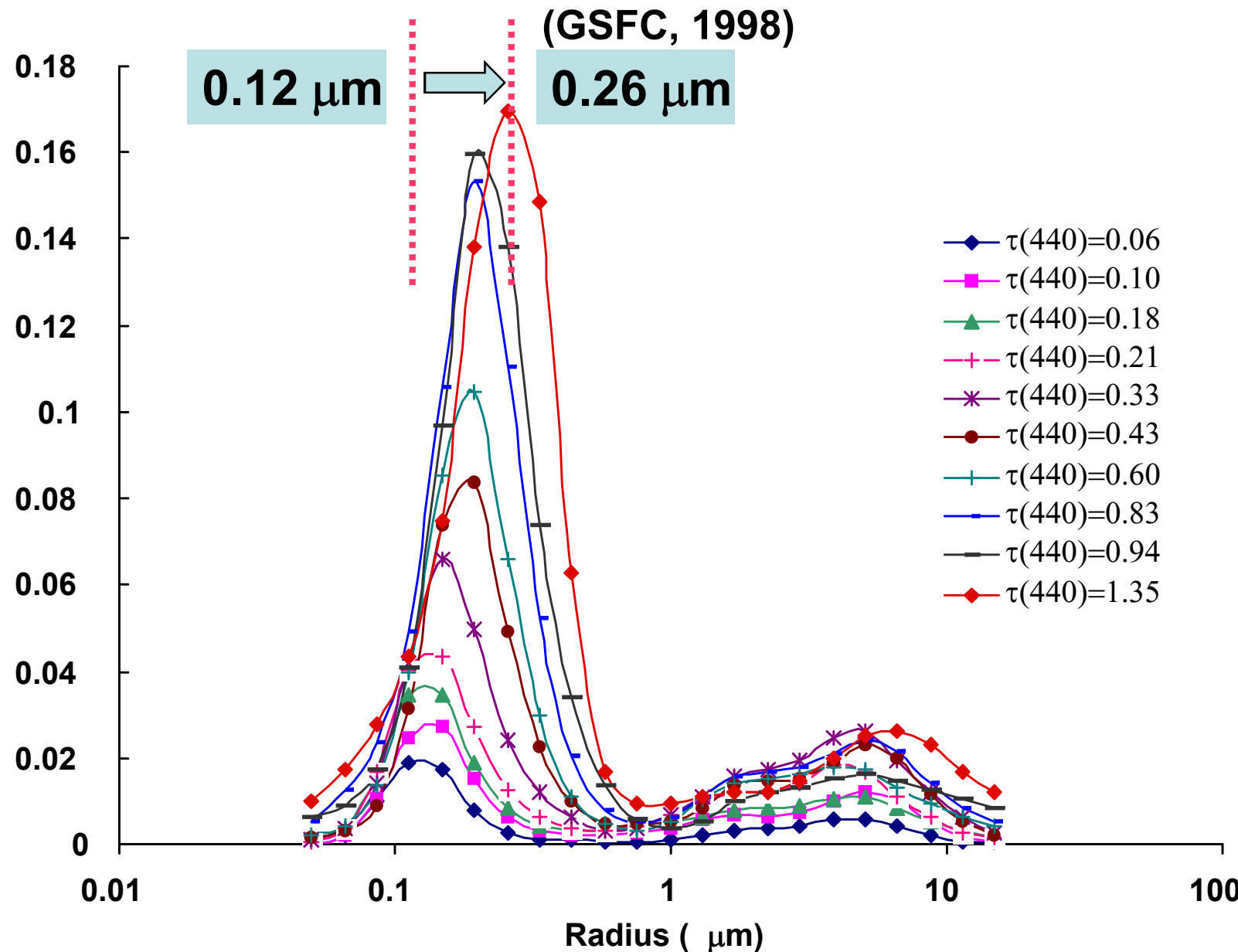


smoldering combustion  
Quebec fires, July 2002



## Variability of particle size distribution

(GSFC, 1998)



# Maritime aerosol



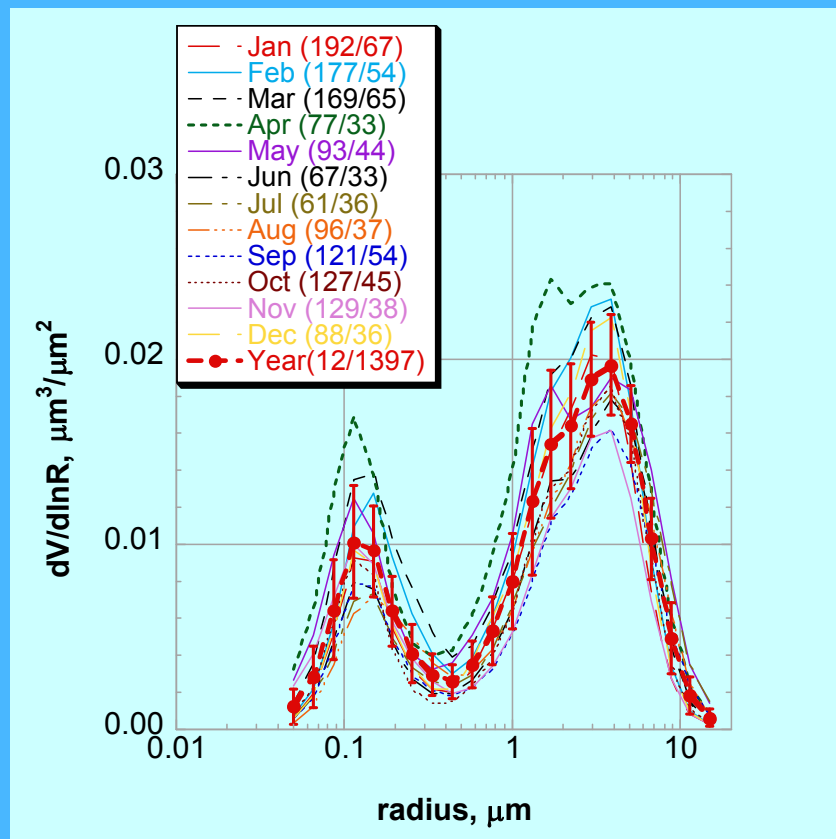
Marcello Bartinetti  
“Sea storm in Camogli”



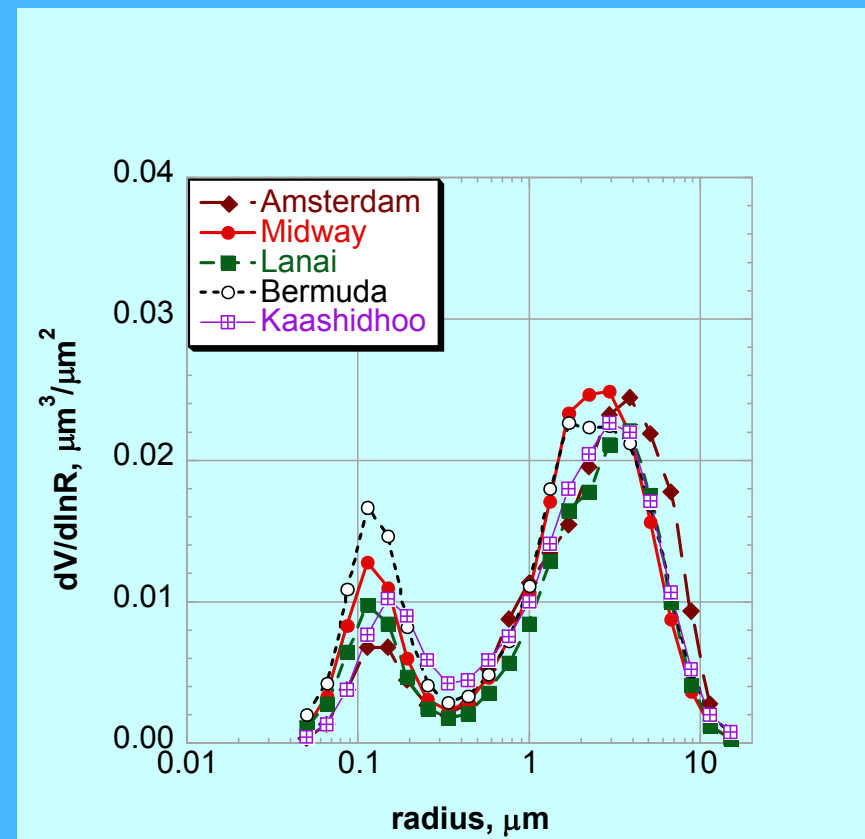
Duck, North Carolina, March 1999

# Oceanic aerosol

Lanai, Hawaii



Worldwide locations



# AERONET estimated broad-band fluxes in solar spectrum

$$F_{\text{broadband}} = \int_{\lambda_{\min}}^{\lambda_{\max}} F(\lambda) d\lambda$$

## ***Integrations details:***

- ✓  $\lambda_{\min} = 0.2 \mu\text{m}$ ,  $\lambda_{\max} = 4.0 \mu\text{m}$ ;
- ✓ more than 200 points of integration between;

## **Aerosol:**

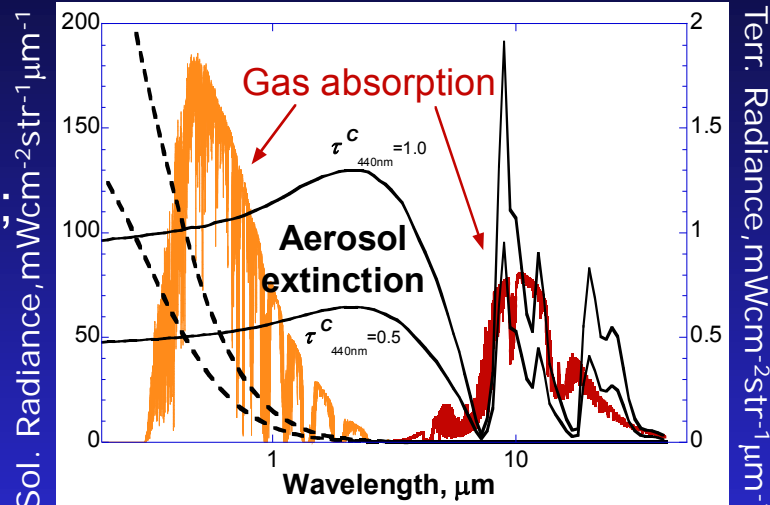
- ✓  $dV/d\ln R$  - retrieved
- ✓  $n(\lambda)$  and  $k(\lambda)$  are interpolated/extrapolated;  
from  $n(\lambda_i)$  and  $k(\lambda_i)$  retrieved;
- ✓ Radiative transfer code uses 12 moments for  $P_{11}(\Theta)$

## **Surface:**

- ✓ Surface reflection is Lambertian;
- ✓ Values of surface reflectance are interpolated/ extrapolated from MODIS data values

## **Gases:**

- ✓ Gaseous absorption is calculated using correlated  $k$ -distributions implemented by P. Dubuisson



***Validation studies:***  
Derimian et al. 2008  
Garcia et al. 2008  
( $F_{\text{BOA}}^{\downarrow} \sim 10\%$  agreement )

# Rigorous ERRORS estimates: Dubovik 2004

## General case: large number of unknowns and redundant measurements

$$\langle (\Delta \hat{x}_i)^2 \rangle \approx \langle (\Delta \hat{x}_i^{random})^2 \rangle + (\Delta \hat{x}_i^{bias})^2$$

$$C_{\Delta \hat{x}^{random}} = \left( \mathbf{U}^T \mathbf{C}^{-1} \mathbf{U} + \mathbf{U}_a^T \mathbf{C}_a^{-1} \mathbf{U}_a \right)^{-1}$$

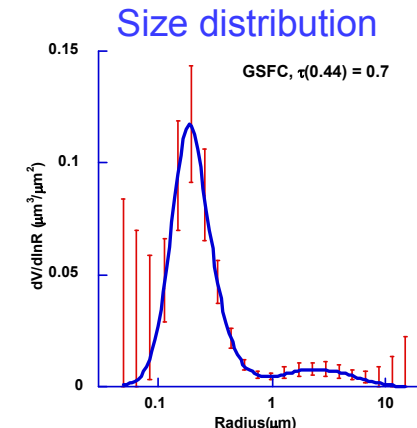
$$\Delta \hat{x}^{bias} = \left( \mathbf{U}^T \mathbf{C}^{-1} \mathbf{U} + \mathbf{U}_a^T \mathbf{C}_a^{-1} \mathbf{U}_a \right)^{-1} \left( \mathbf{U}^T \mathbf{C}^{-1} \Delta \mathbf{I}^{bias} + \mathbf{U}_a^T \mathbf{C}_a^{-1} \Delta \mathbf{I}_a^{bias} \right)$$

$\mathbf{U}$  - matrix of partial derivatives in the vicinity of solution  $\hat{\mathbf{x}}$

Above is valid:

- in linear approximation
- for Normal Noise
- strongly dependent on a priori constraints
- very challenging in most interesting cases

# Input ERRORS and biases



Random (normally distributed with 0 means):

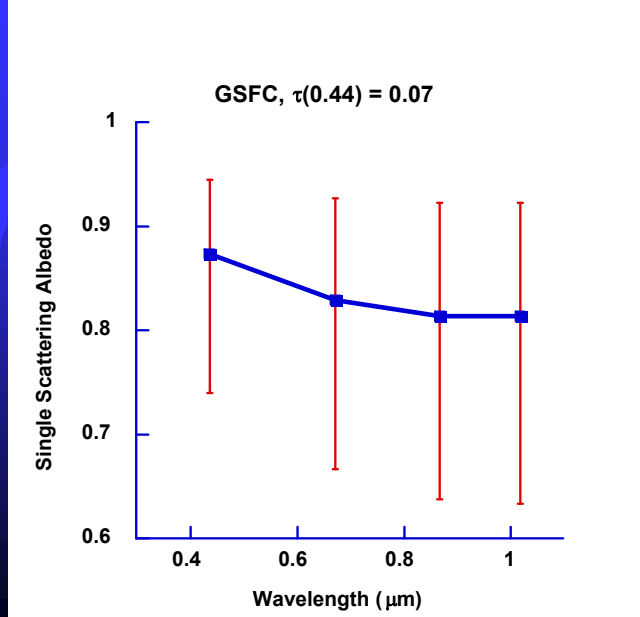
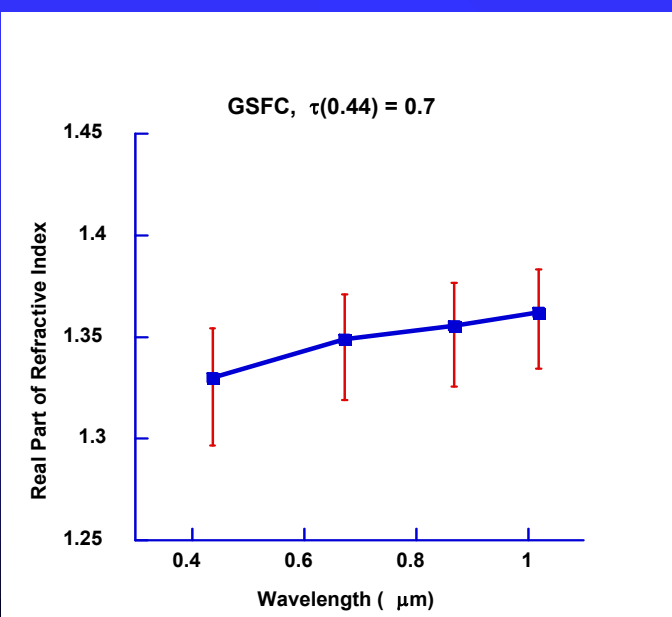
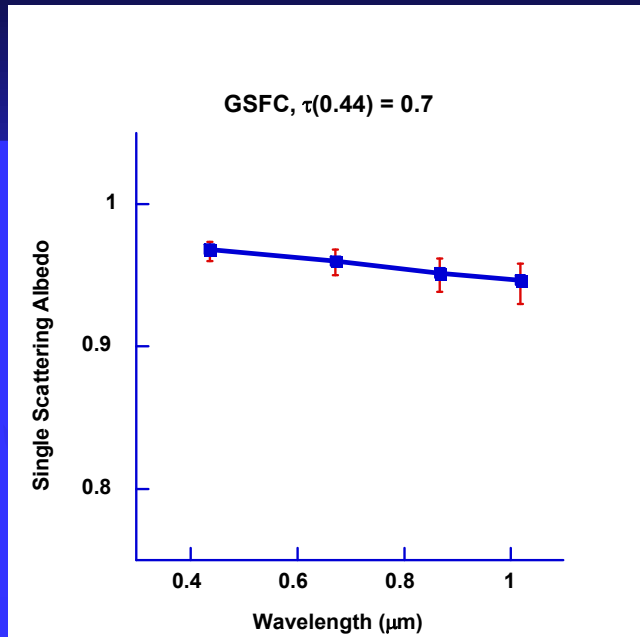
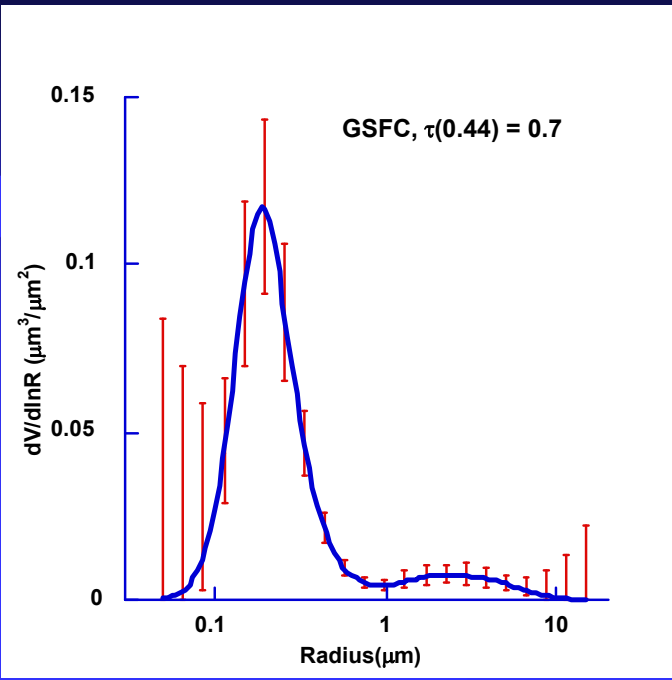
- optical thickness:  $\sigma_\tau = 0.015 \times \text{COS(SZA)}$
- sky-radiances:  $\sigma_{\text{sky}} = 3\%$
- a priori:  $\sigma_{\text{sky}} / \gamma_i \sim 100 - 300\% \text{ (Dubovik and King, 2000)}$

Biases (constant):

- optical thickness:  $\pm 0.015 \times \text{COS(SZA)}$
- sky-radiances:  $\pm 3\% + \text{obtained misfit}$
- a priori:  $100 - 300\%$

The error estimates are calculated twice with + and - bias.

# Examples of error estimates



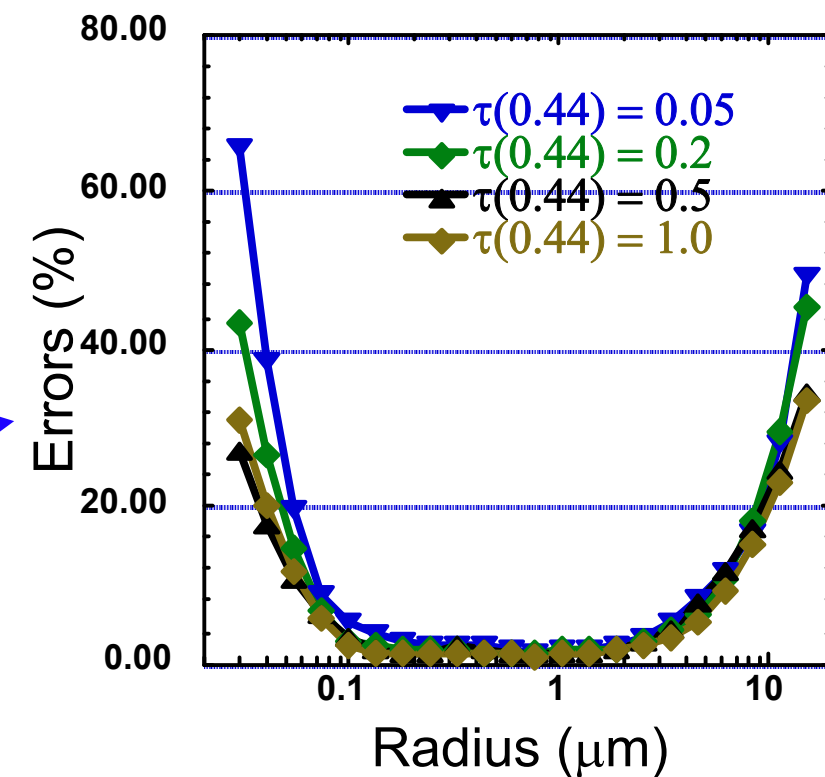
# Random ERRORS in AERONET retrievals

## ASSUMPTIONS:

- measurements have Normal Noise:
  - optical thickness:  $\sigma = 0.01$
  - sky-radiances:  $\sigma = 5\%$

## CONCLUSIONS:

- the retrievals stable
- important tendencies outlined





# Sensitivity to instrumental offsets

## Offsets were considered in:

- optical thickness:  $\Delta\tau(\lambda) = \pm 0.01; \pm 0.02;$
- sky-channel calibration:  $\Delta_I(\lambda; \Theta)/I(\lambda; \Theta) 100\% = \pm 5\%;$
- azimuth angle pointing:  $\Delta\phi = 0.5^\circ; 1^\circ;$
- assumed ground reflectance:  $\Delta A(\lambda)/A(\lambda) 100\% = \pm 30\%; \pm 50\%;$

## Aerosol models considered (bi-modal log-normal):

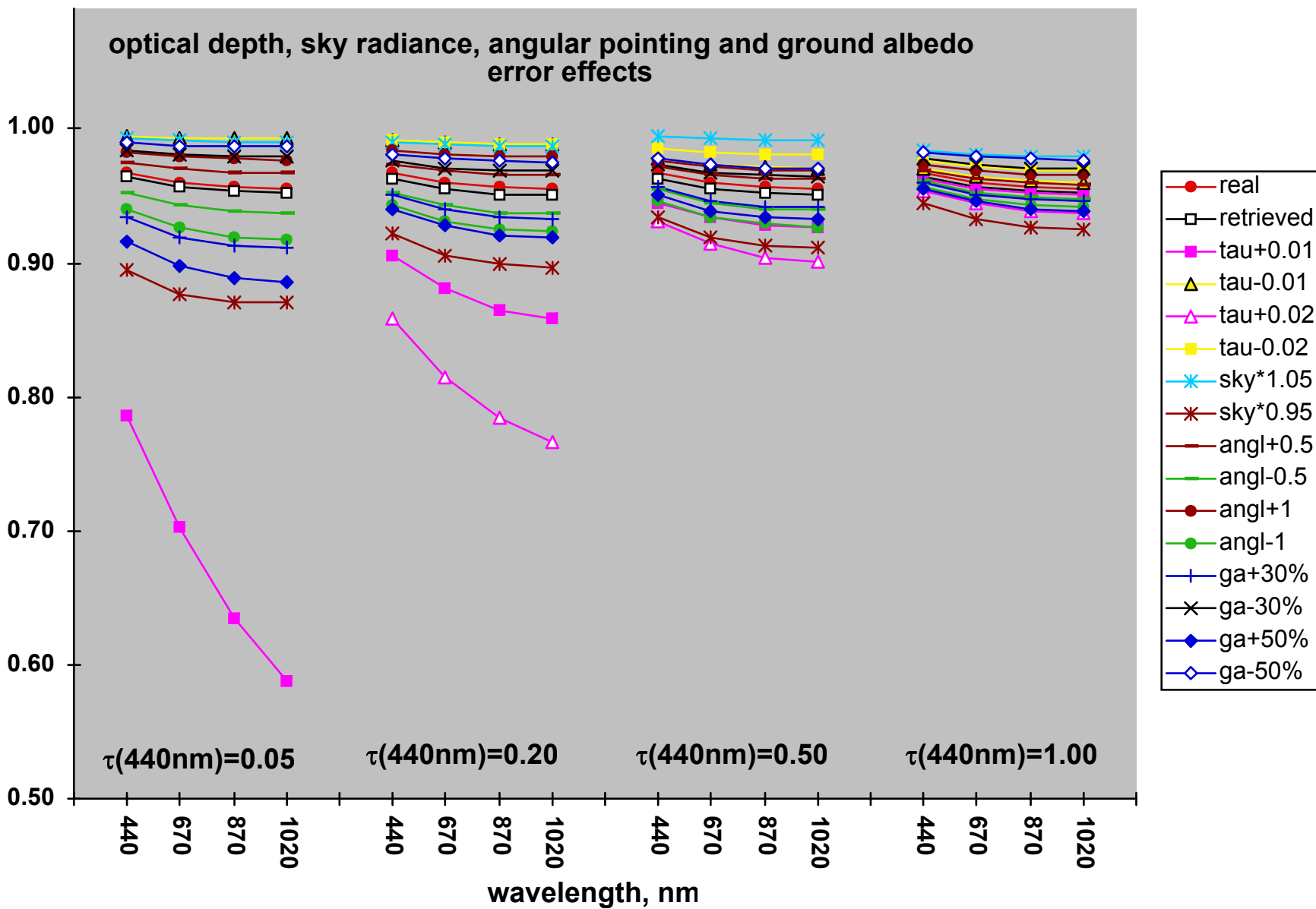
- Water-soluble aerosol for  $0.05 \leq \tau(440) \leq 1;$
- Desert dust for  $0.5 \leq \tau(440) \leq 1;$
- Biomass burning for  $0.5 \leq \tau(440) \leq 1;$

## Results summary:

- $\tau(440) \leq 0.2$  -  $dV/d\ln r$  (+),  $n(\lambda)$  (-),  $k(\lambda)$  (-),  $\omega_0(\lambda)$  (-)
- $\tau(440) > 0.2$  -  $dV/d\ln r$  (+),  $n(\lambda)$  (+),  $k(\lambda)$  (+),  $\omega_0(\lambda)$  (+)
- Angular pointing accuracy is critical for  $dV/d\ln r$  of dust

(+) **CAN BE** retrieved

(-) **CAN NOT BE** retrieved



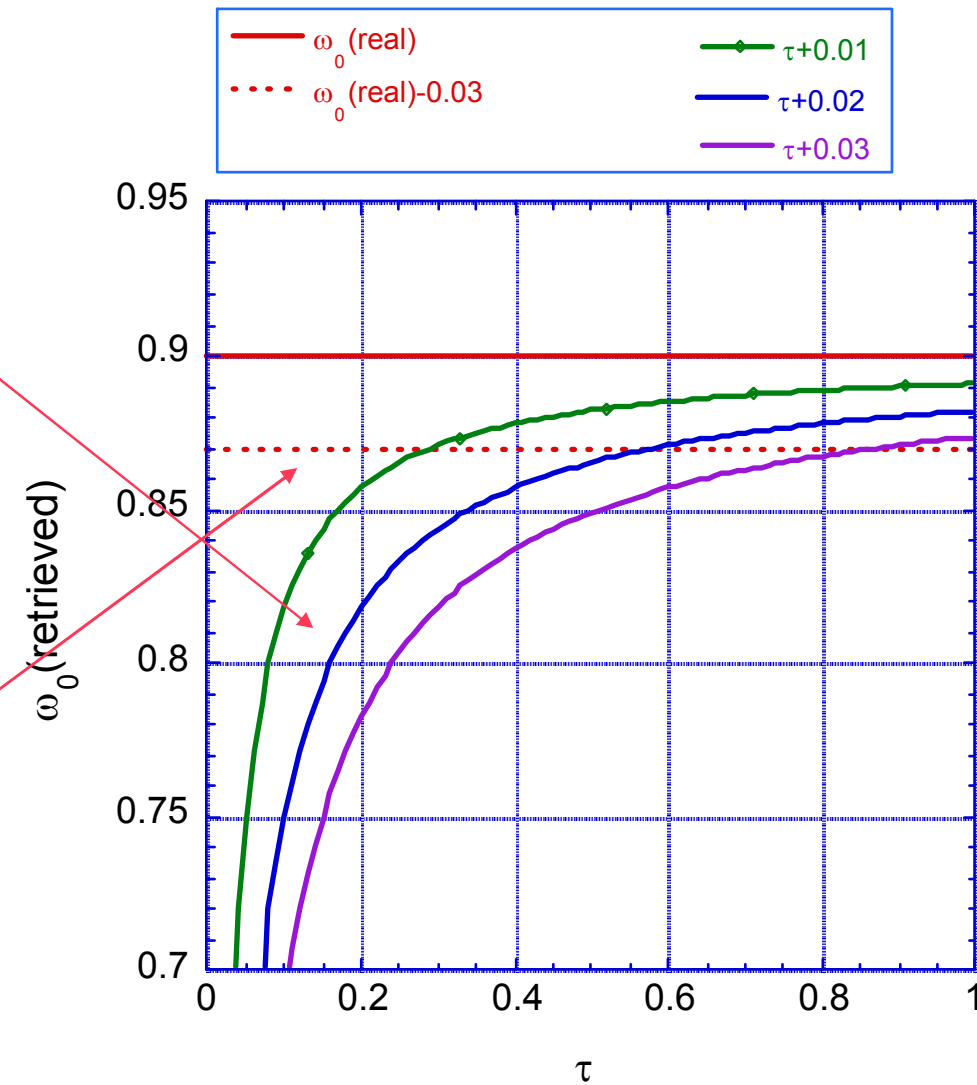
# $\Delta\tau$ bias influence at $\Delta\omega_0$

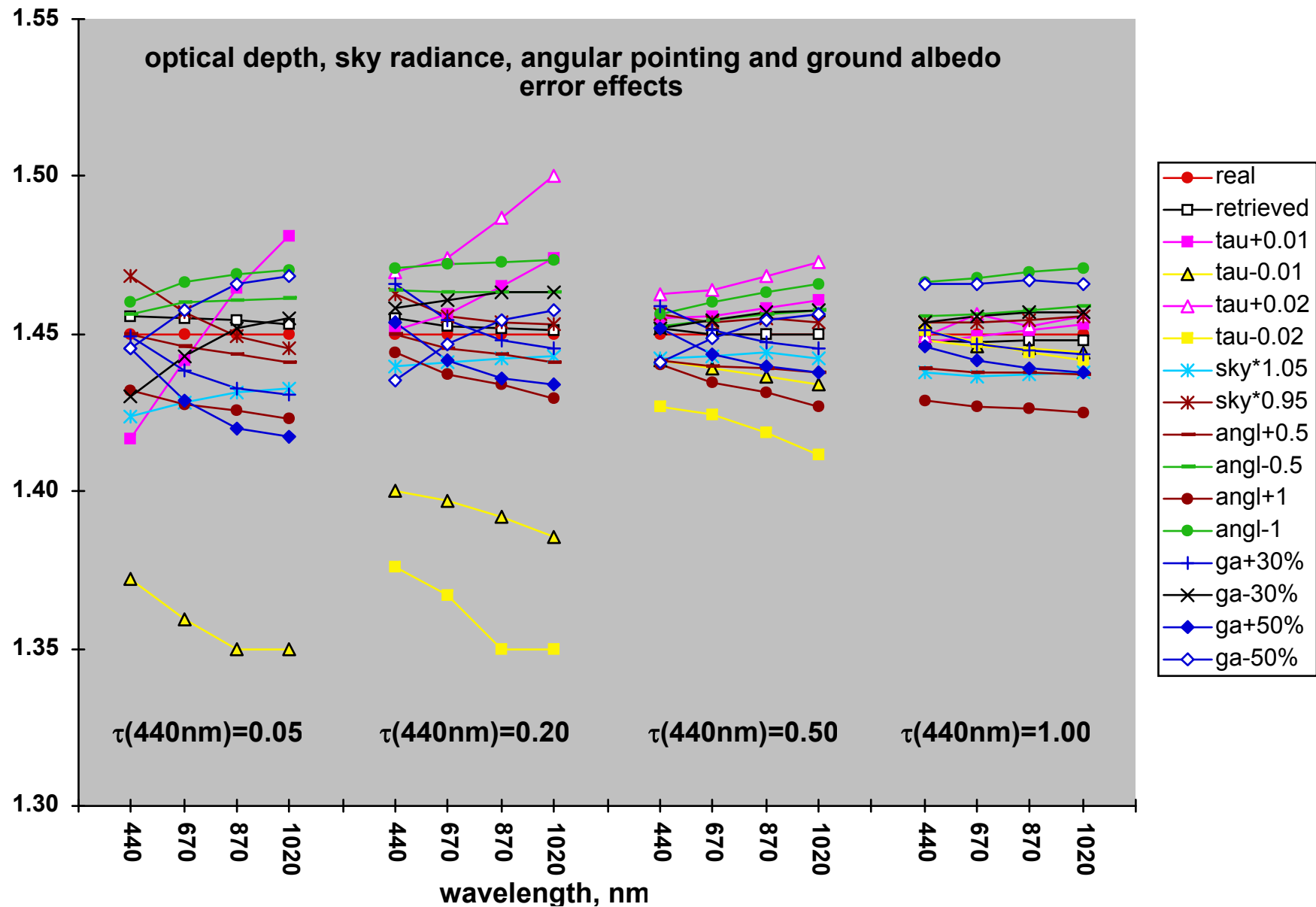
**$\Delta\tau$  bias:**

$$\tilde{\omega}_0 = \frac{\tau_{scat}}{\tau_{ext} + \Delta\tau}$$

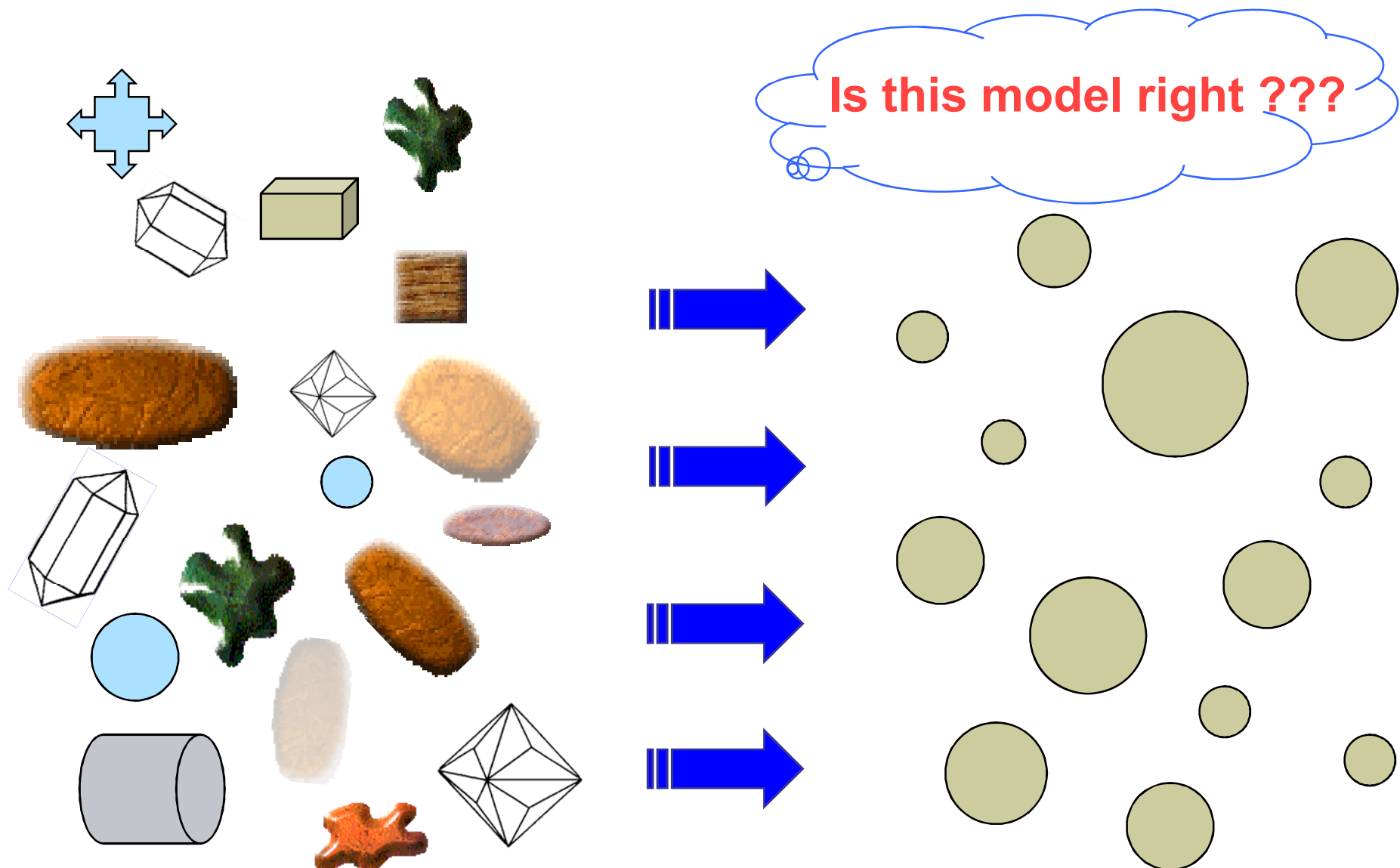
**Sky Radiance bias:**

$$\tilde{\omega}_0 = \frac{\tau_{scat} (1 - \Delta)}{\tau_{ext}}$$
$$= \omega_0 (1 - \Delta)$$



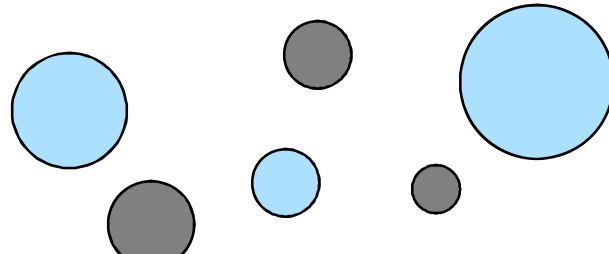


# Optical model of aerosol

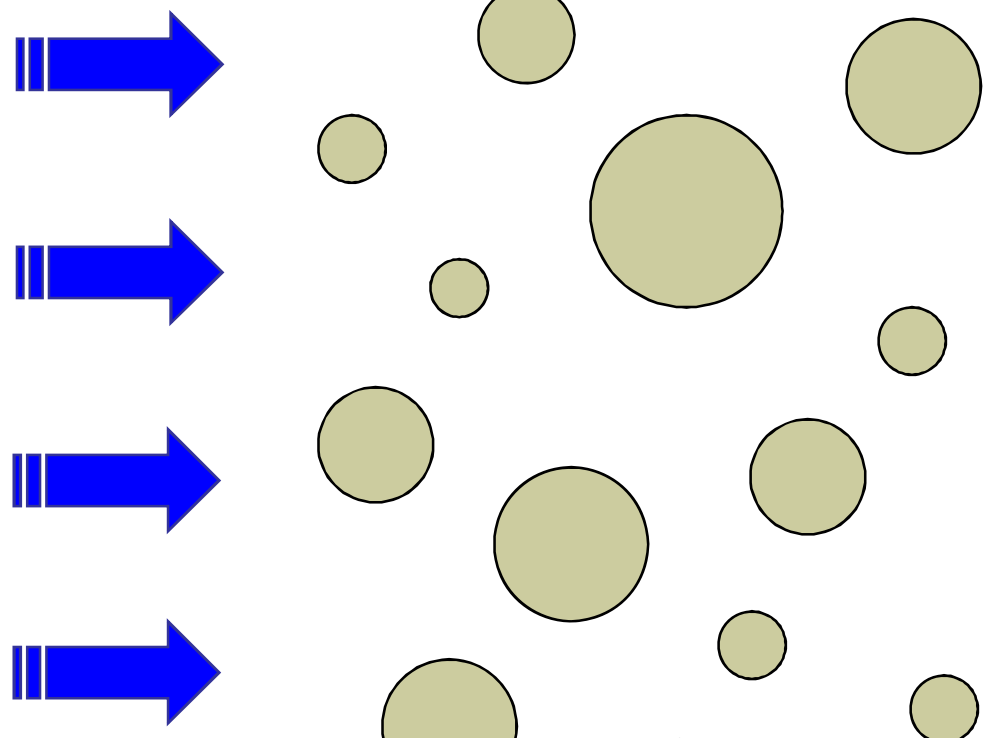


# Questioned simplifications:

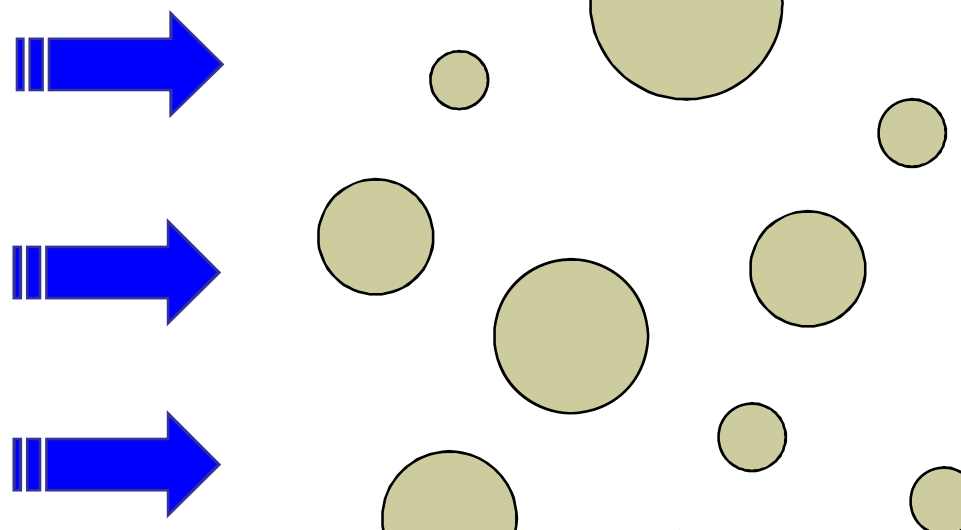
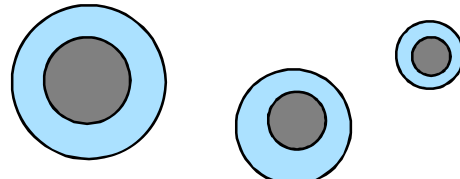
"external" mixture:



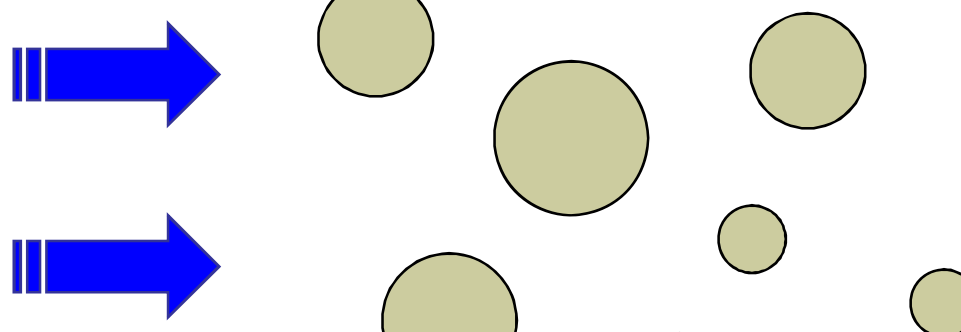
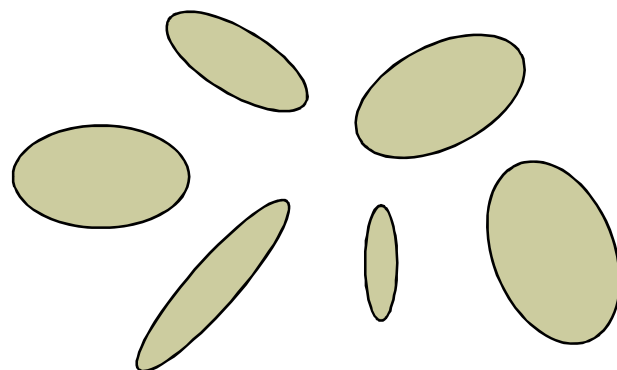
Is, at least, this right ???



"internal" mixture:



non-sphericity:





# Sensitivity to forward model limitations

## Mixed aerosols (inhomogeneous spherical aerosols):

- Externally mixed ( $n(l)$  and  $k(l)$  different for fine and coarse modes)
- Internally mixed ( $n(l)$  and  $k(l)$  different for core and shell) - *Biomass Burning*

### *Results summary:*

- $dV/dlnr$  (+),  $\omega_0(\lambda)$  (+),  $n(\lambda)$  (+, effective),  $k(\lambda)$  (+, effective)

## Non-spherical aerosols:

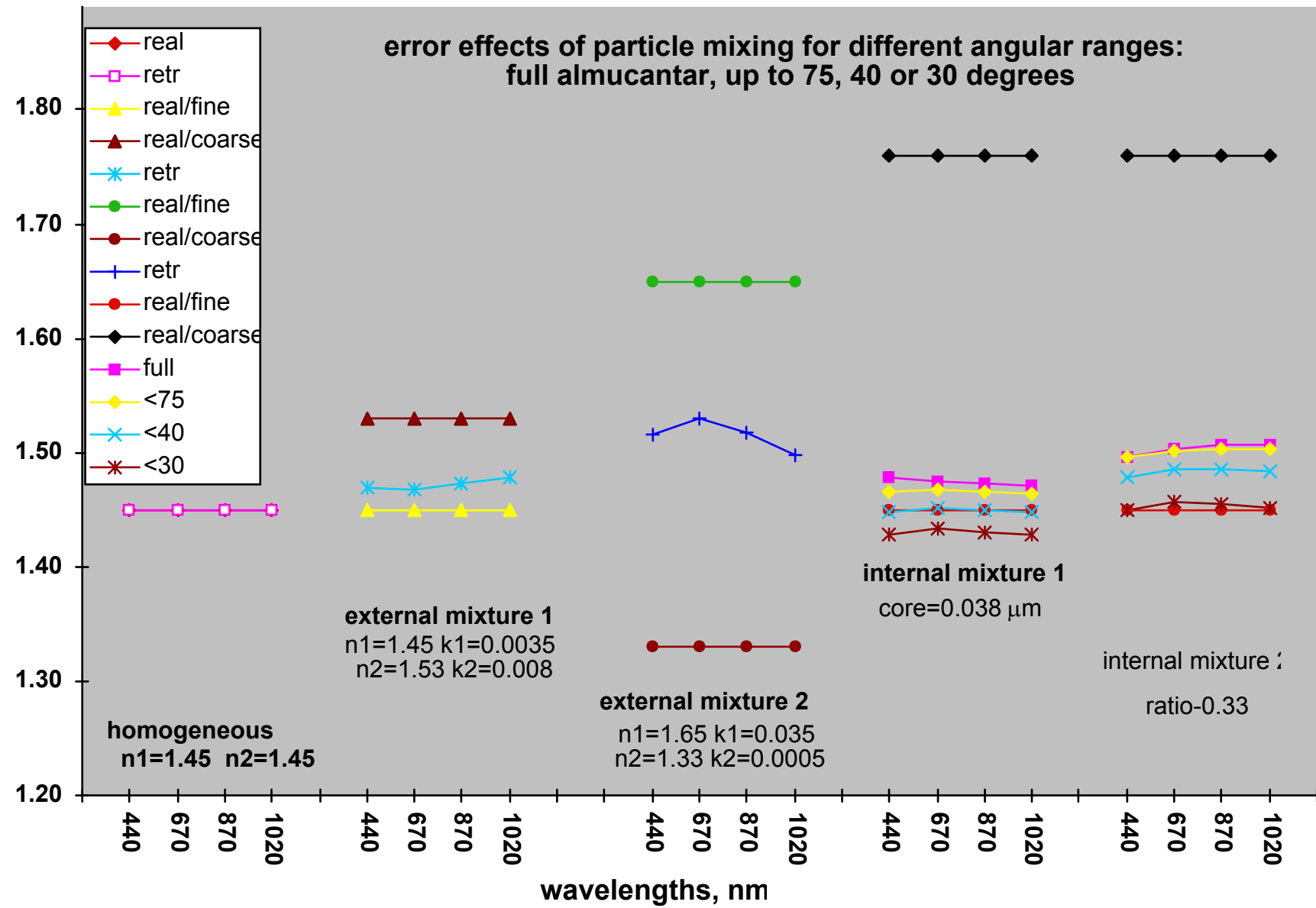
- Spheroids (prolate, axis ratio 2) - *Desert dust*

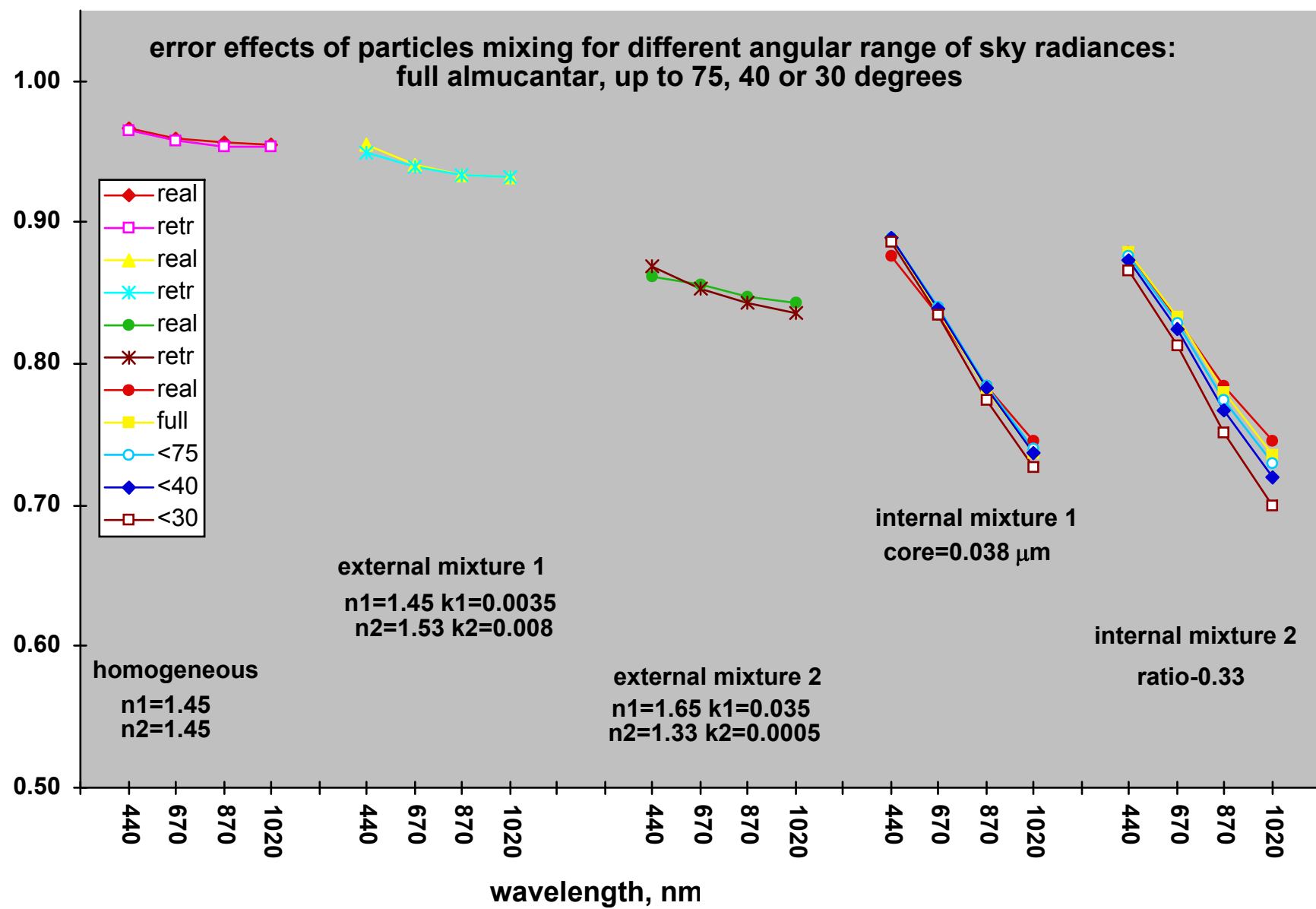
### *Results summary:*

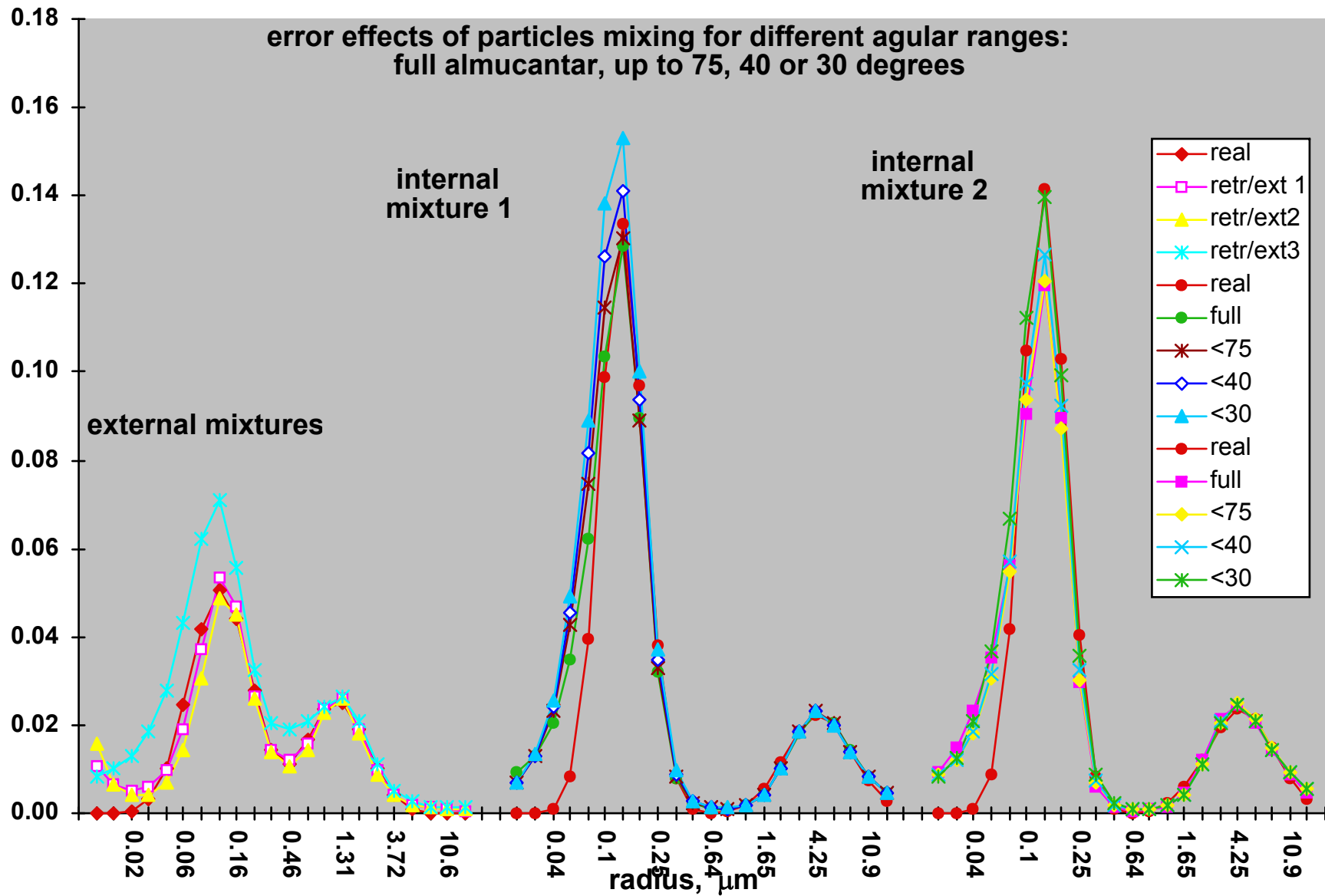
- $dV/dlnr$  - coarse mode (+), fine mode (+, zenith angle  $< 25^\circ$ )
- $\omega_0(\lambda)$  (+) - full solar almucantar (zenith angle  $\geq 50^\circ$ )
- $k(\lambda)$  (+)
- $n(440)$  (-),  $n(670)$  (-),  $n(870)$  (+/-),  $n(1020)$  (+)

(+) CAN BE retrieved

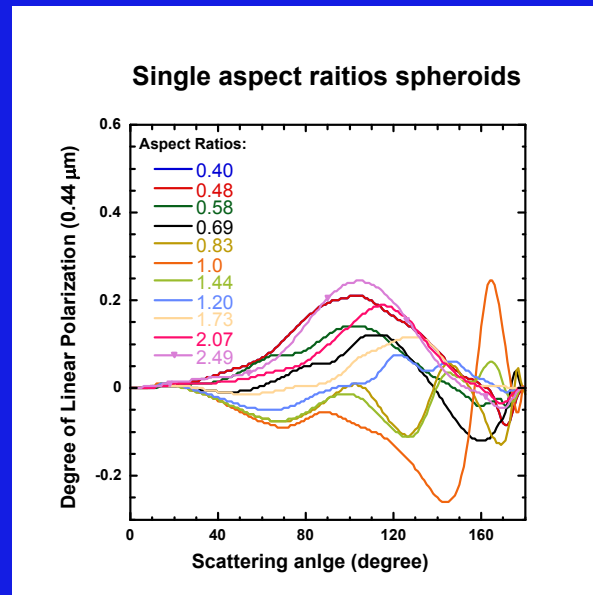
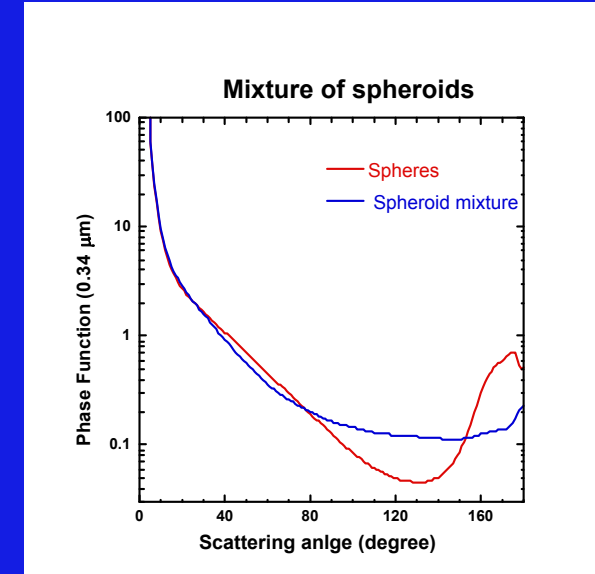
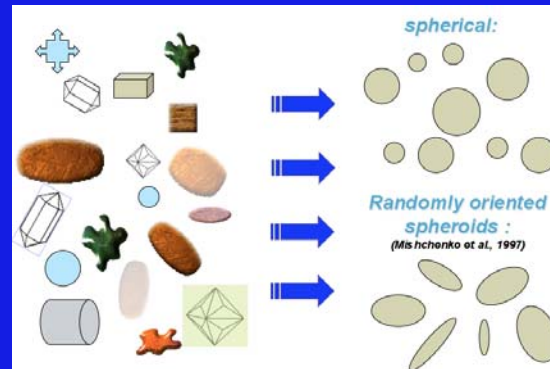
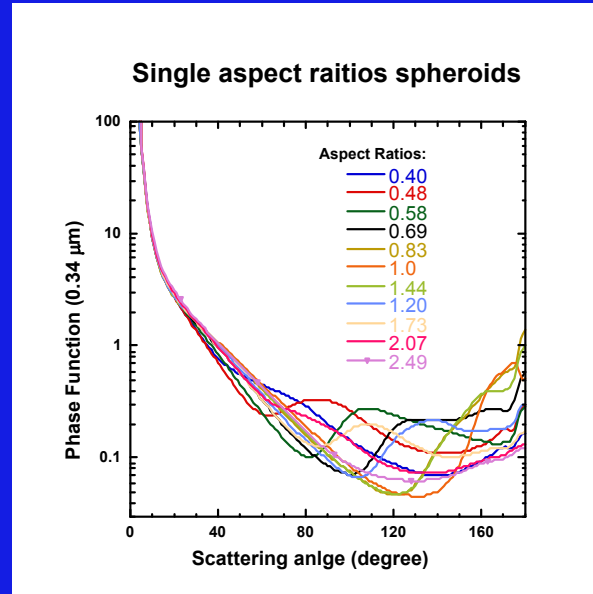
(-) CAN NOT BE retrieved



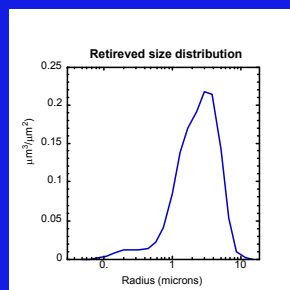
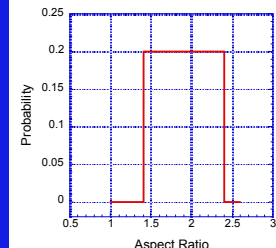




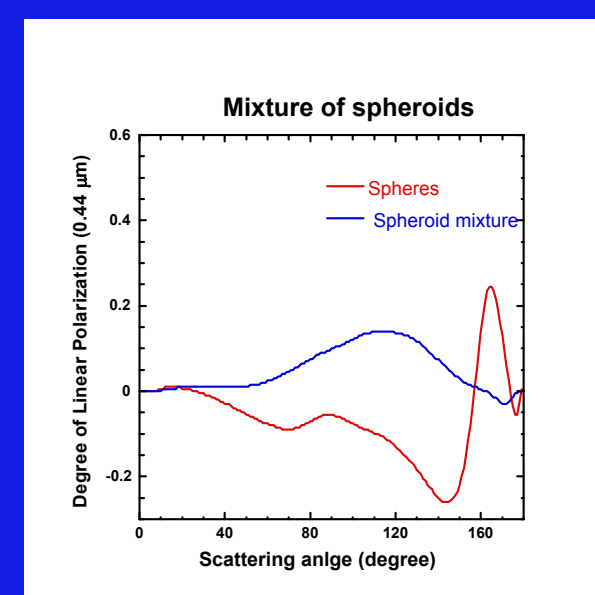
# Modeling Dust particle non-sphericity



Averaging with  $\omega(\varepsilon)$

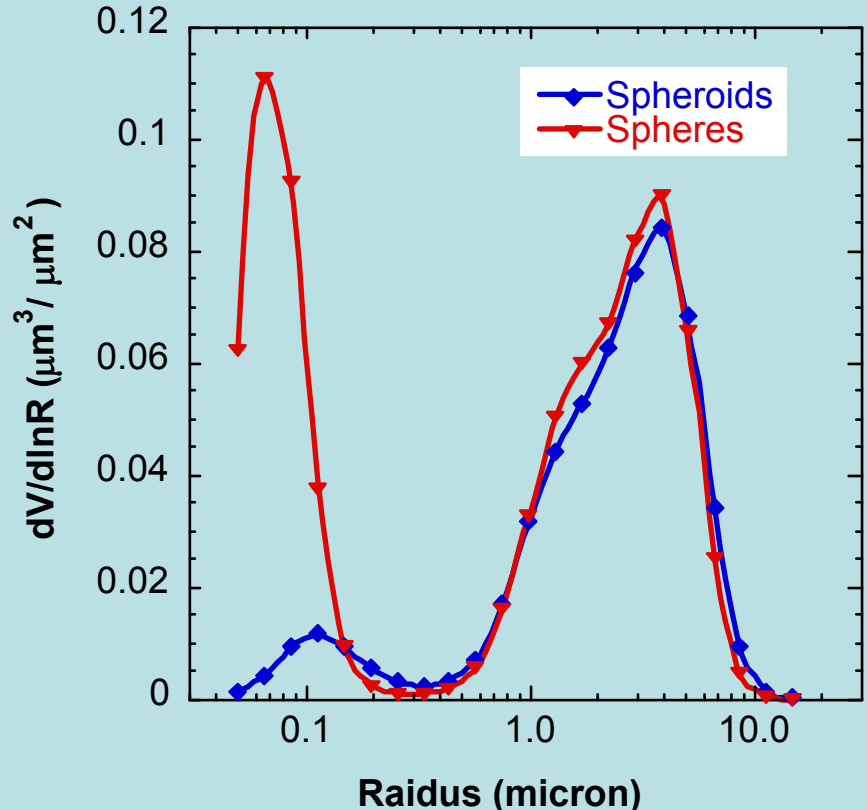


$n(\lambda)$        $k(\lambda)$

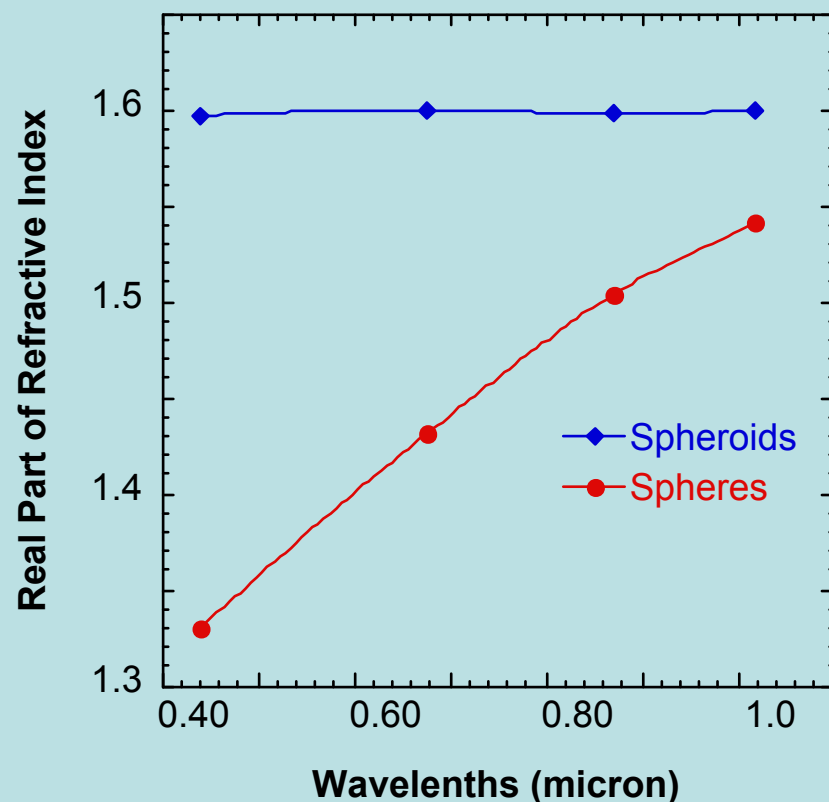


# Artifacts in AERONET retrievals caused by non-sphericity of Desert Dust particles

Effect of shape assumptions on retrieved dust size distribution



Influence of shape assumption on retrieved ref. index



# Retrieval accuracy and limitations

Sensitivity tests by  
Dubovik et al. 2000

Effective

wide angular  
coverage

Real Part

Imaginary Part

SSA

bias  $\Delta\tau = \pm 0.01$

$$\tau(0.44) \leq 0.2$$

$$0.05$$

$$80-100\%$$

$$0.05-0.07$$

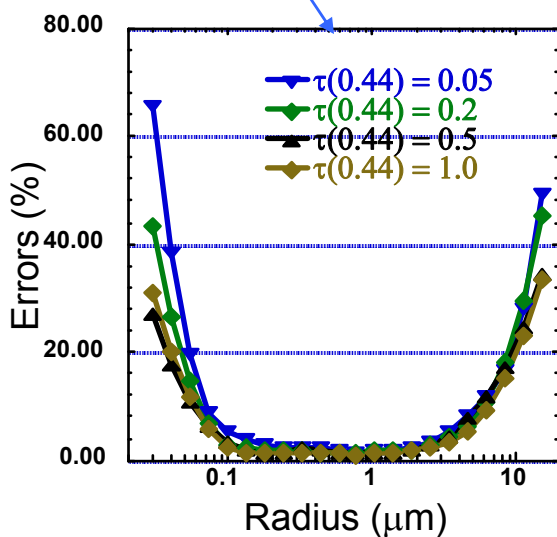
$$\tau(0.44) \geq 0.5$$

$$0.025$$

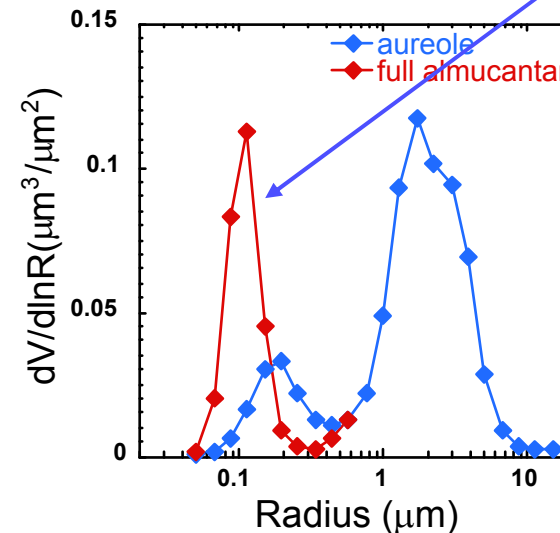
$$50\%$$

$$0.03$$

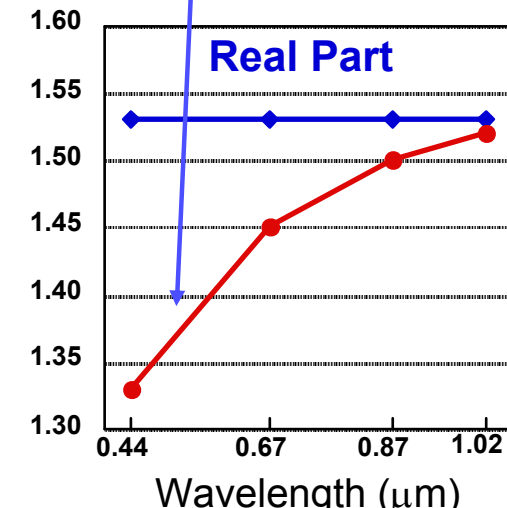
Random errors



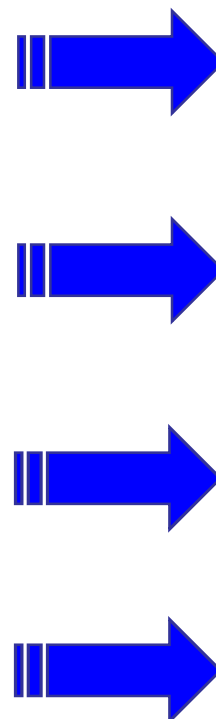
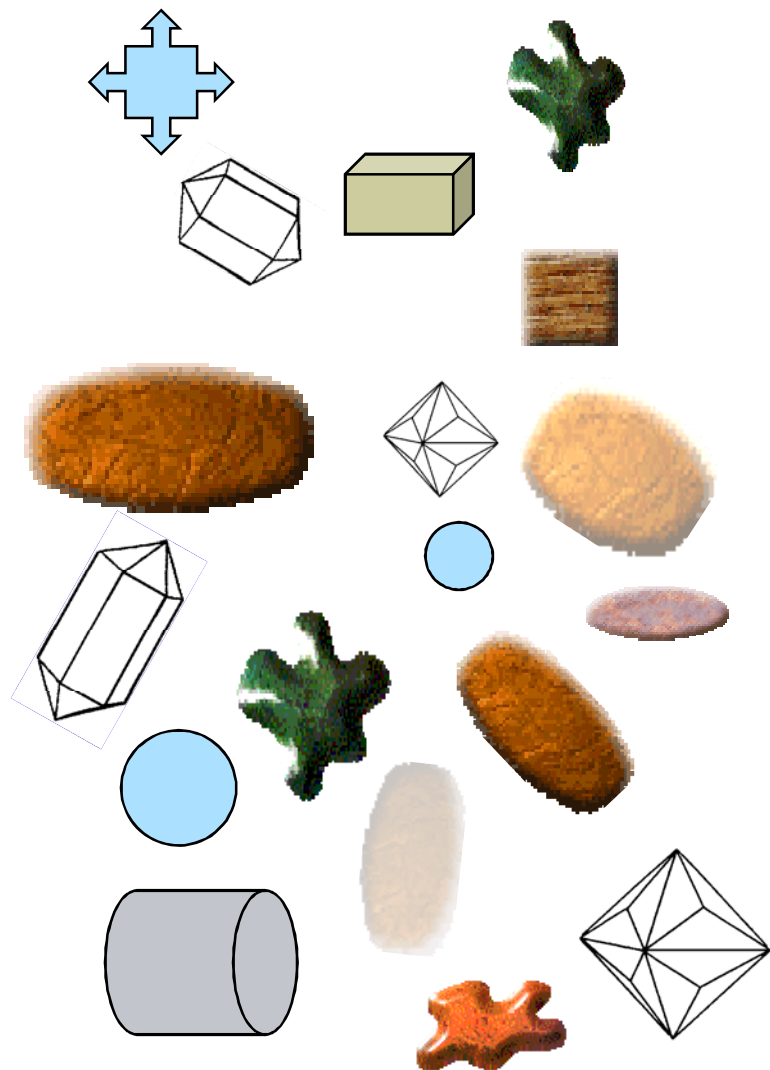
Size Distribution:



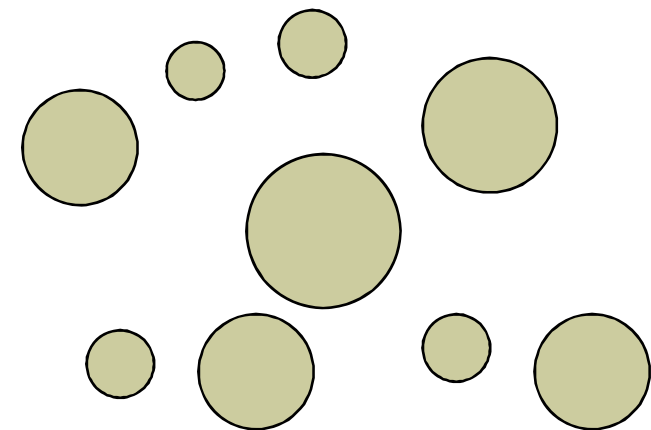
Nonsphericity  
biases



# AERONET model of aerosol

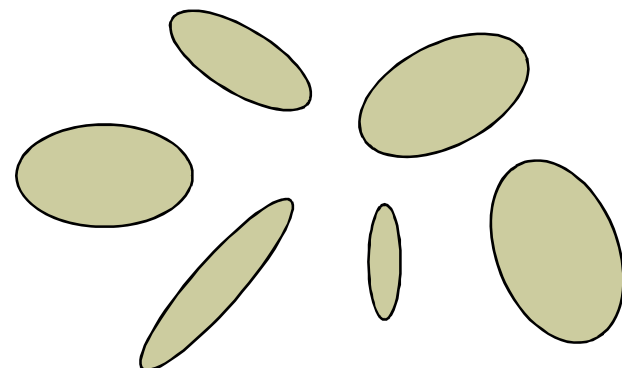


*spherical:*



*Randomly oriented  
spheroids :*

*(Mishchenko et al., 1997)*



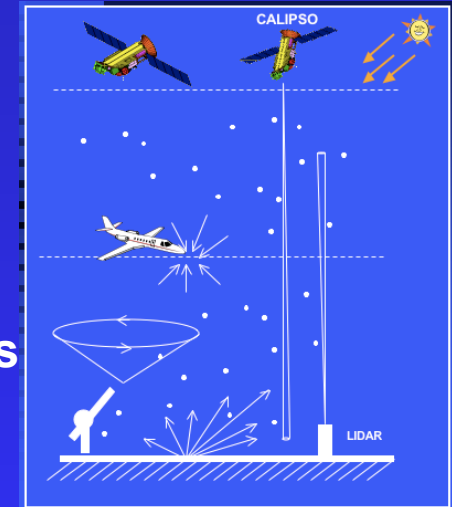


# CONCLUSIONS:



## 1. Achivements:

- the retrieval is rather elaborated;
- the retrieval provides not only the main set of parameters but also extended set secondary products;
- the results are provided together with error estimates
- the model and accuracy is verified in sensitivity studies
- useful climatologies were developed;



## 2. Perspectives:

- more efficient use of polarimetric measurements
- updating model of non-spherical fraction
- deriving aerosol composition
- combining photometric data with other co-incident observations

# AERONET retrieval products:



- V1



- V2



- V3

## *Directly retrieved parameters:*

- $dV/d\ln R$  - size distribution; (- dynamic errors )
- $C(t,f,c)$ ,  $R_v(t,f,c)$ ,  $\sigma(t,f,c)$ ,  $R_{\text{eff}}(t,f,c)$  - integral parameters of  $dV/d\ln R$
- $n(\lambda)$  and  $k(\lambda)$  at 0.44, 0.67, 0.8, 1.02  $\mu\text{m}$ ; (- dynamic errors )
- $C_{\text{spherical}}$  - fraction of spherical particles (- dynamic errors )

## *Indirectly retrieved/estimated parameters:*

### ♣ popular:

- $\omega_0$  - at 0.44, 0.67, 0.8, 1.02  $\mu\text{m}$ ; (- dynamic errors )
- $P_{11}(\Theta, \lambda)$  (- dynamic errors ) and  $\langle \cos(\Theta) \rangle$  ;
- $P_{12}(\Theta, \lambda)$  and  $P_{22}(\Theta, \lambda)$  - ??? (- dynamic errors )
- $F_{\text{TOA}}^{\downarrow}(\lambda)$  and  $F_{\text{BOA}}^{\downarrow}(\lambda)$  - down ward spectral fluxes
- $F_{\text{TOA}}^{\uparrow}(\lambda)$  and  $F_{\text{BOA}}^{\uparrow}(\lambda)$  - upward spectral fluxes

### ♣ not well-known / under-developed:

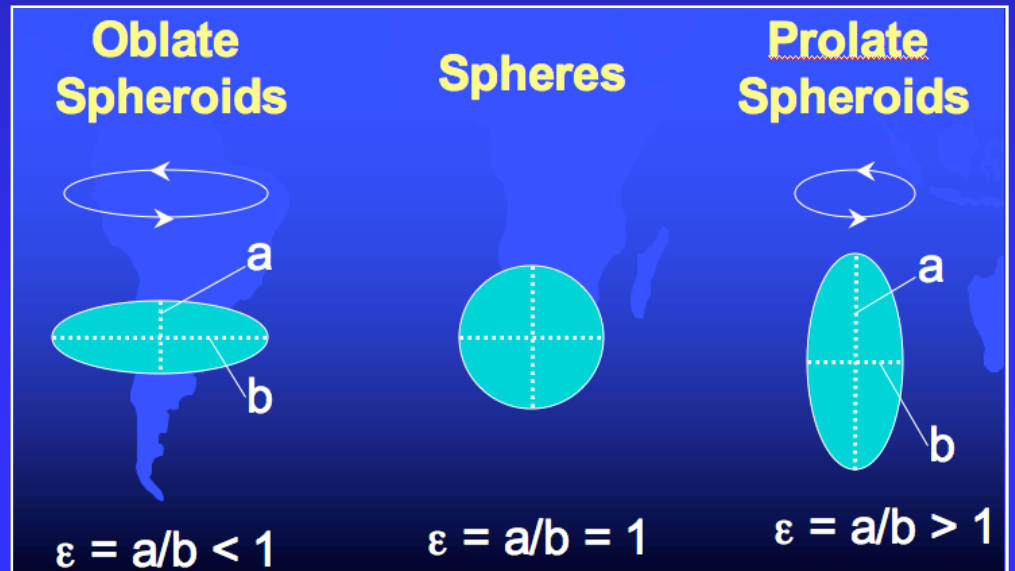
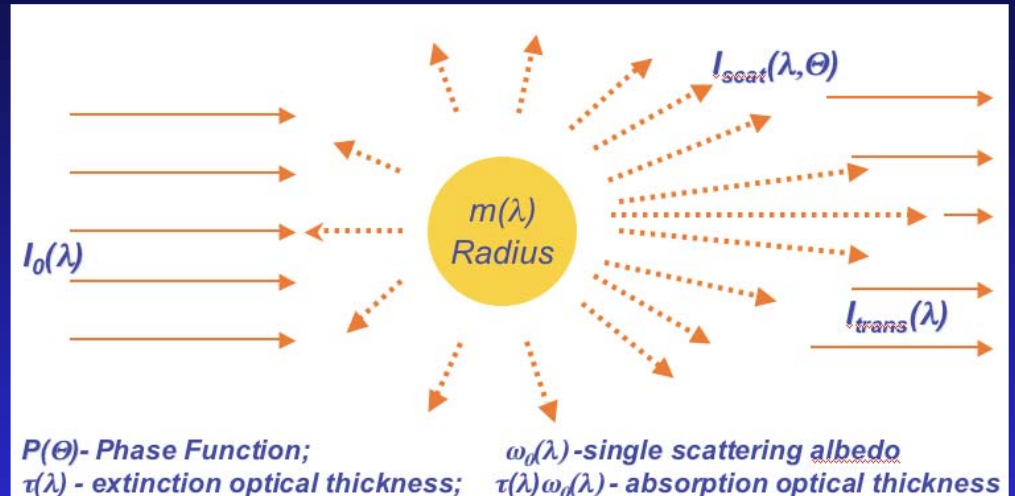
- $S(\lambda)$  - lidar backscattering-to-extinction ratio; (- dynamic errors )
- $\delta(\lambda)$  - lidar depolarization ratio ; (- dynamic errors )
- $F_{\text{TOA}}^{\downarrow}$  and  $F_{\text{BOA}}^{\downarrow}$  - down ward broad-band (visible) fluxes;
- $F_{\text{TOA}}^{\uparrow}$  and  $F_{\text{BOA}}^{\uparrow}$  - upward broad-band (visible) fluxes;
- $\Delta F_{\text{TOA}}$  and  $\Delta F_{\text{BOA}}$  - radiative forcing
- $\Delta F_{\text{TOA}}^{\text{Eff}}$  and  $\Delta F_{\text{BOA}}^{\text{Eff}}$  - radiative forcing efficiency

# Aerosol single particle scattering:

ASSUMPTIONS in  
the retrievals:

EACH AEROSOL PARTICLE

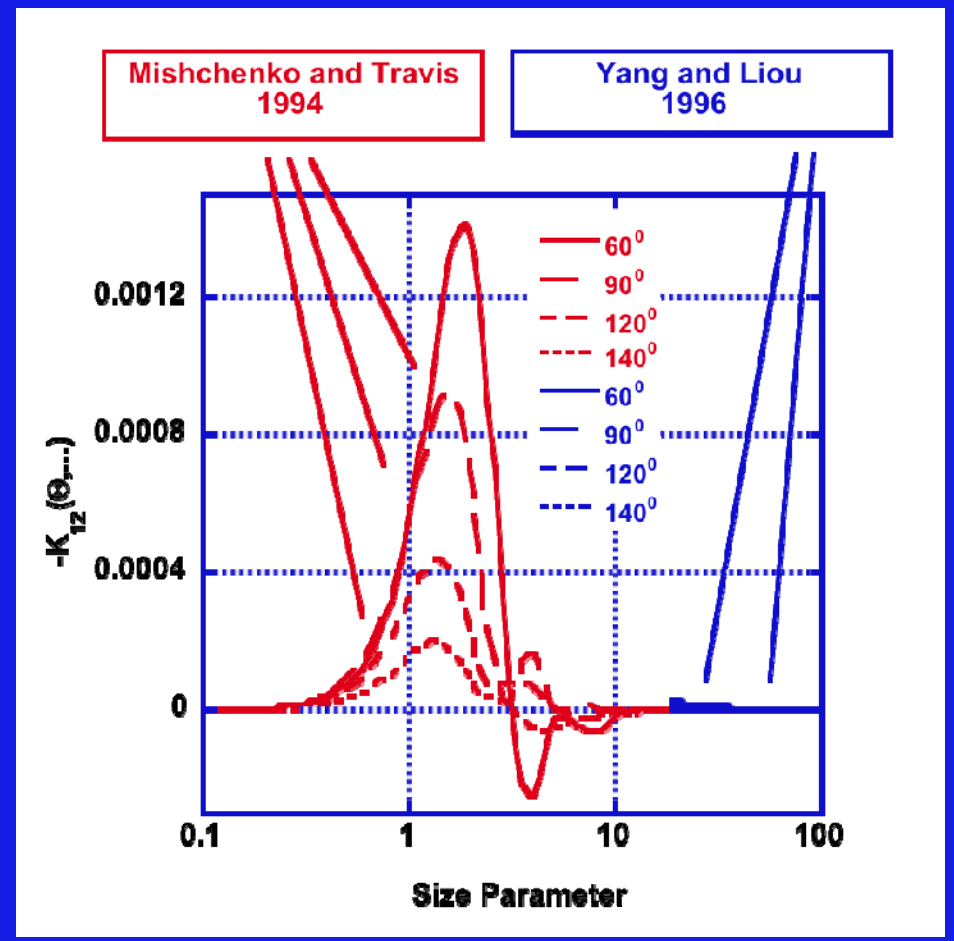
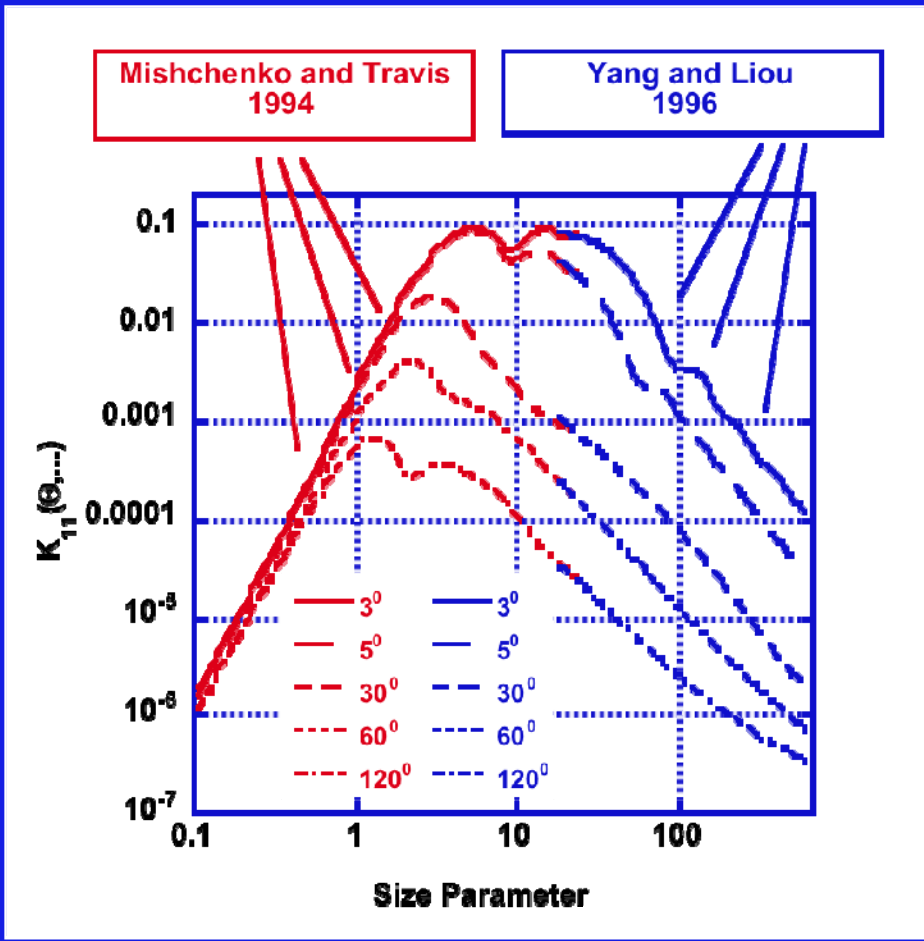
- sphere or spheroid (!!!);
- homogeneous;
- $1.33 \leq n \leq 1.7$
- $0.0 \leq k \leq 0.5$
- $n$  and  $k$  spectrally dependent  
*(but smooth)*



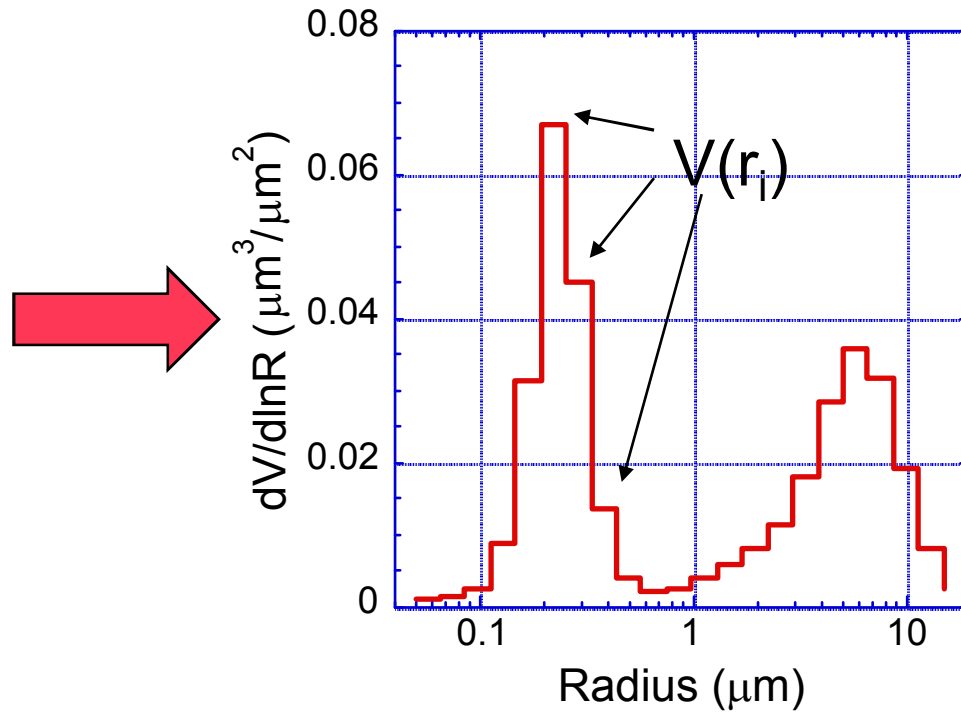
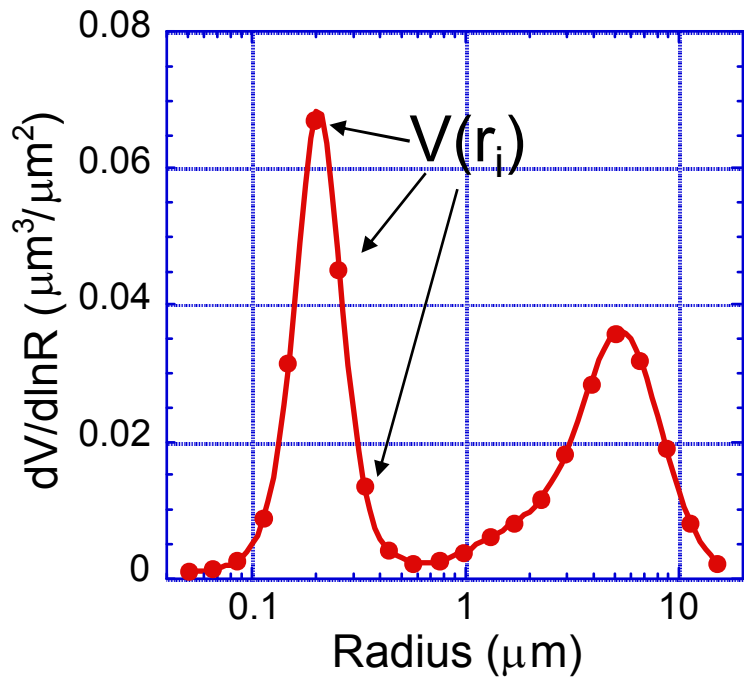
# *Computational challenge of using spheroids model*

Strategy: using two complementary methods

Example for prolate spheroids with aspect ratio  $\sim 2.75$



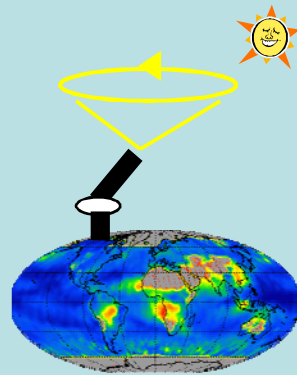
# Modeling Spheroid Polydispersions



$$\tau(\lambda) = \int_{\varepsilon_{\min}}^{\varepsilon_{\max}} \int_{r_{\min}}^{r_{\max}} K_\tau(\lambda; k; n; \varepsilon; r) N(\varepsilon) V(r) dr d\varepsilon \approx \sum_j \sum_i N(\varepsilon_j) V(r_i) \int_{r_i - \Delta/2}^{r_i + \Delta/2} K_\tau(\lambda; k; n; \varepsilon_j; r_i)$$

$K(\lambda; k; n; \varepsilon_j; r_i)$

- Kernel look-up table for fixed  $r_i$  (22 points)  
 $(1.33 \leq n \leq 1.7; 0.0 \leq k \leq 0.5, 0.3 \leq \varepsilon \leq 3.0)$



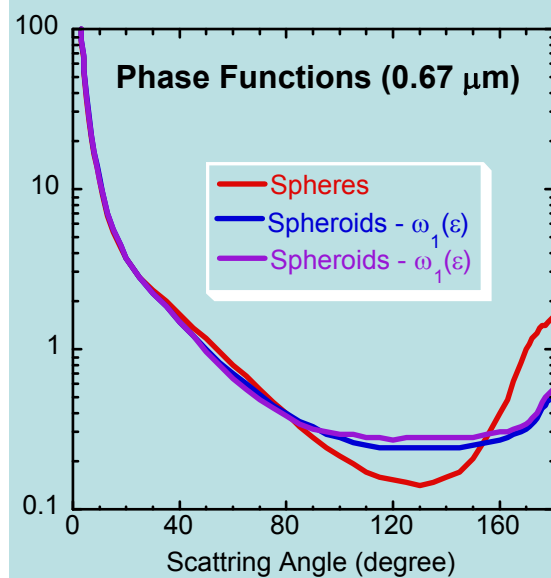
# spheroid kernels data base for operational modeling !!!

Basic Model by Mishchenko et al.  
1997:  
 ➤ randomly oriented  
 homogeneous spheroids  
 ➤  $\omega(\varepsilon)$  - size independent shape  
 distribution

**K** - pre-computed  
 kernel matrices:  
 Input: n and k

**Input:**  $\varepsilon_i$  ( $N_p = 25$ ),  
 $V(r_i)$  ( $N_i = 22 - 41$ )

$$\tau(\lambda), F_{11}, \dots, F_{44} \approx \sum_{(i,p)} K_{ip}(\dots; \lambda; n; k) N(\varepsilon_p) V(r_i)$$



**Time:** < one sec.  
**Accuracy:** < 1-3 %  
**Range of applicability:**  
 $0.012 \leq 2\pi r/\lambda \leq 625$  (41 bins)  
 $0.3 \leq \varepsilon \leq 3.0$  (25 bins)  
 $1.33 \leq n \leq 1.7$   
 $0.0 \leq k \leq 0.5$

**Output:**  $\tau(\lambda), \omega_0(\lambda),$   
 $F_{11}(\Theta), F_{12}(\Theta), F_{22}(\Theta),$   
 $F_{33}(\Theta), F_{34}(\Theta), F_{44}(\Theta)$

Optics  $\longleftrightarrow$  Microphysics

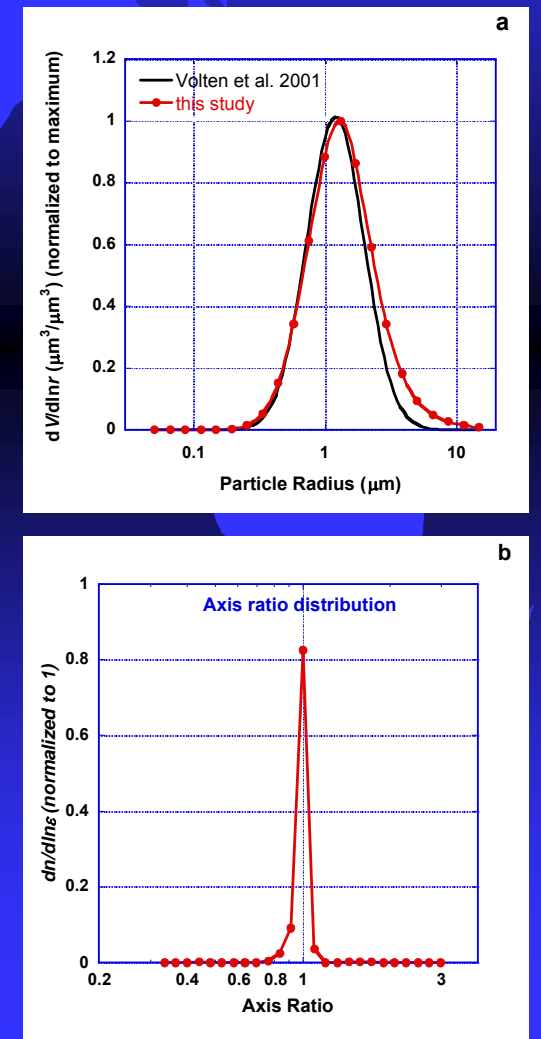
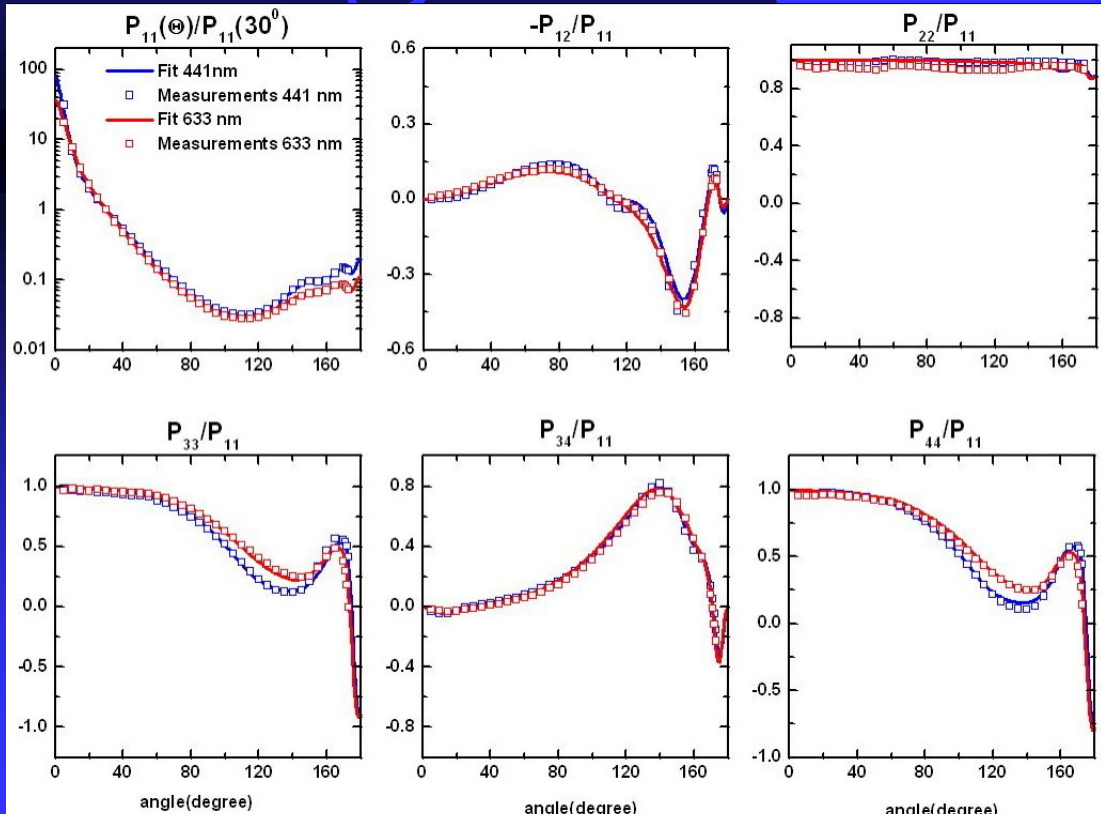
Dubovik et al. (2006)

$$n \approx 1.34-1.35$$

$$k \approx 0.0006 - 0.007$$

## Water Droplets:

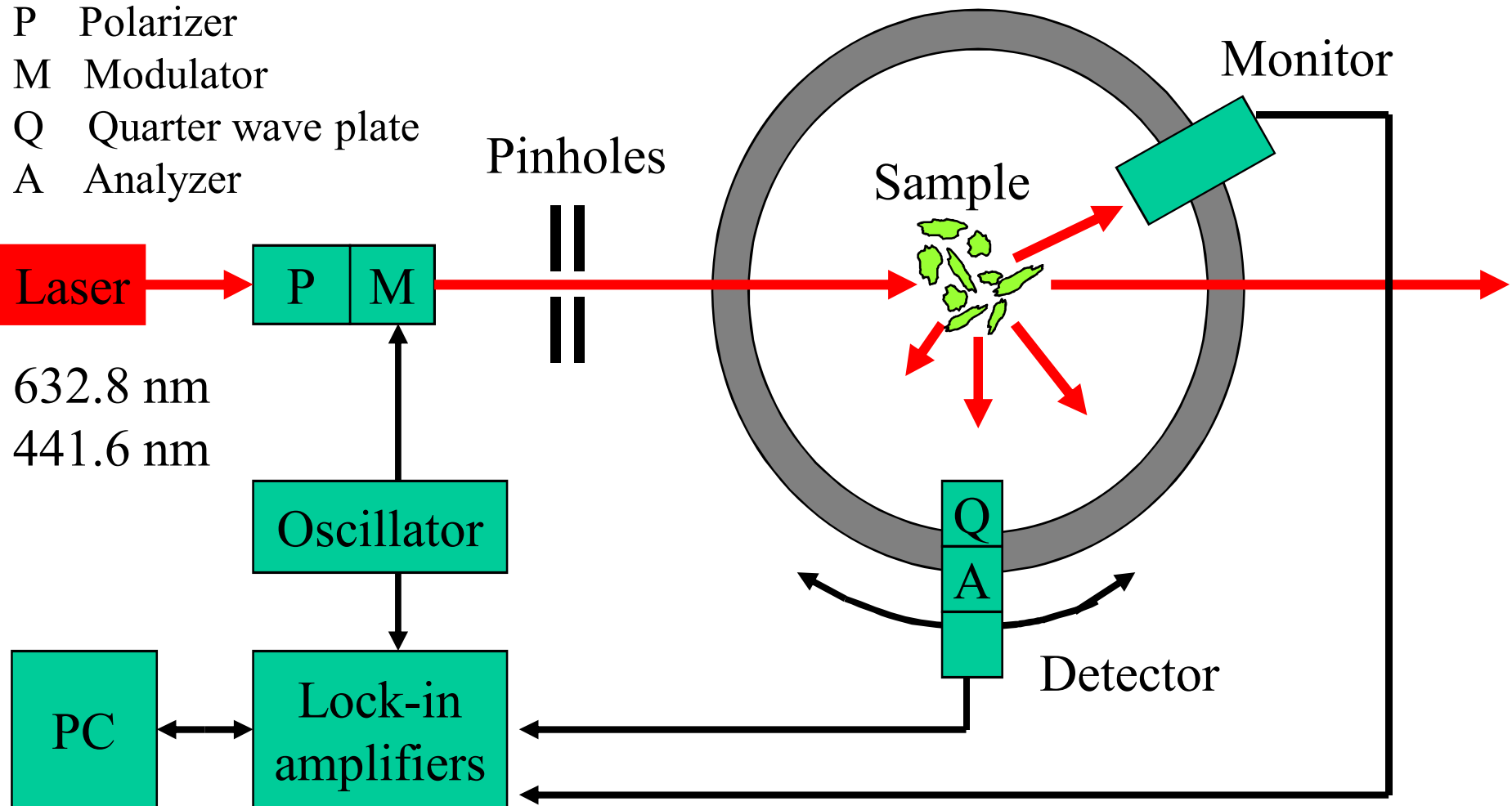
Volten, Munoz et al.



# Measurement

$$\begin{pmatrix} I \\ Q \\ U \\ V \end{pmatrix}_{\text{scatt}} \propto \begin{pmatrix} F_{11} & F_{12} & 0 & 0 \\ F_{12} & F_{22} & 0 & 0 \\ 0 & 0 & F_{33} & F_{34} \\ 0 & 0 & -F_{34} & F_{44} \end{pmatrix} \cdot \begin{pmatrix} I \\ Q \\ U \\ V \end{pmatrix}_{\text{in}}$$

P Polarizer  
M Modulator  
Q Quarter wave plate  
A Analyzer



H. Volten, O. Munoz,  
J. Hovenier,...

## Facts and Figures

**name of sample**

feldspar

**origin**

crushed piece of Feldspar rock from Finland

**main constituents**

K-feldspar, plagioclase, quartz

**particle size**

distributions measured with laser diffraction

$r_{\text{eff}} = 1.0 \text{ micrometer}$ ,  $\nu_{\text{eff}} = 1.0$

**particle shape**

irregular (SEM image)



**refractive index**

estimated to be in the range:  
 $1.5-1.6 - i0.0001-0.00001$

**color**

light pink to white powder



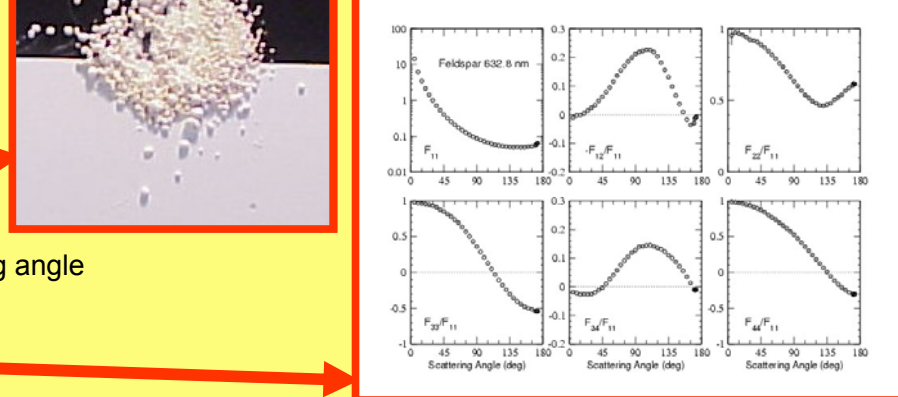
**scattering matrix**

from 5-173 degrees scattering angle

**wavelength**

441.6 nm (figure)

632.8 nm (figure)

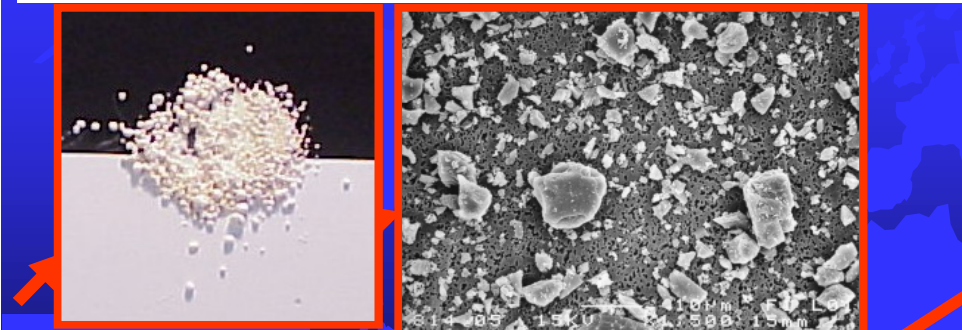


**article**

Scattering matrices of mineral particles at 441.6 nm and 632.8 nm.

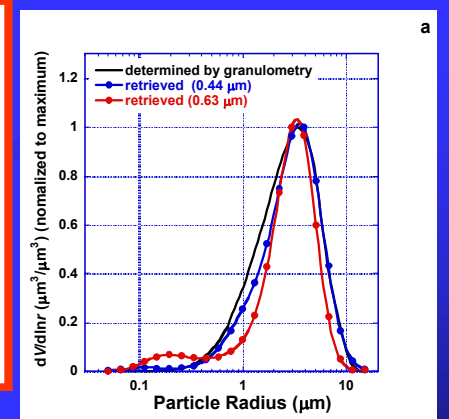
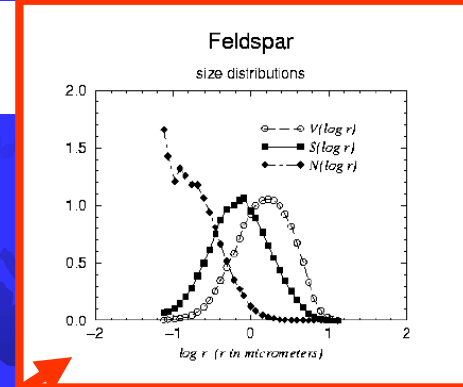
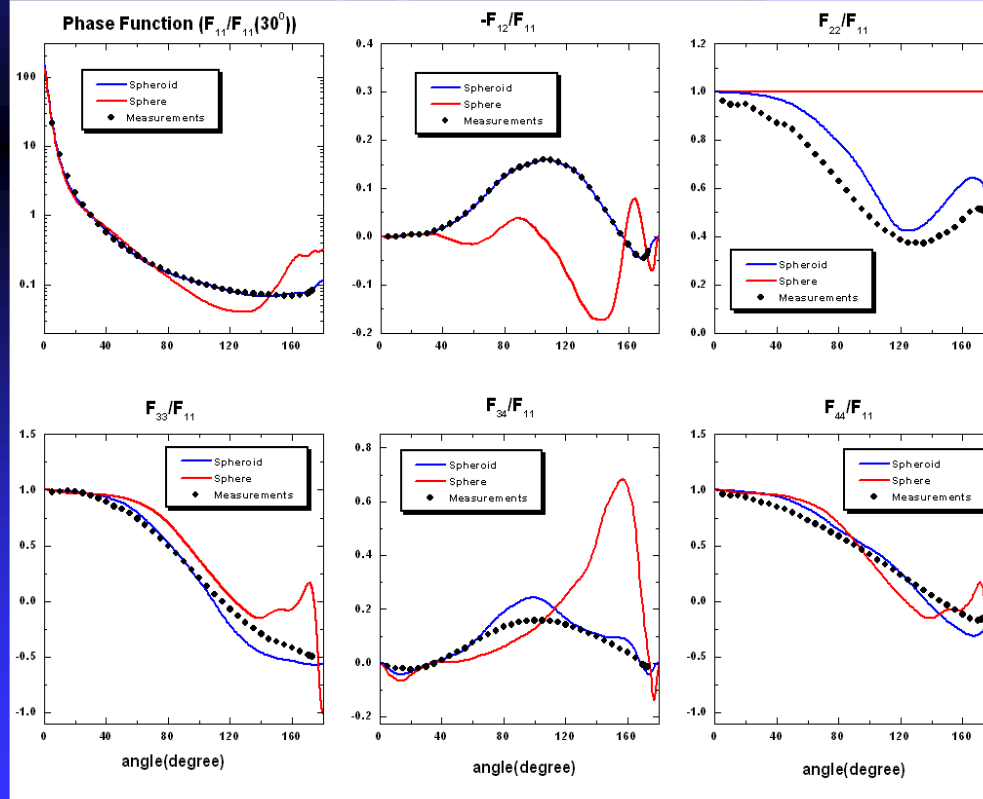
Volten H, Mu-oz O, Rol E, de Haan JF, Vassen W, Hovenier JW, Muinonen K, Nousiainen T.  
Journal of Geophysical Research, 106, 17375-17401, 2001

# Optics ↔ Microphysics



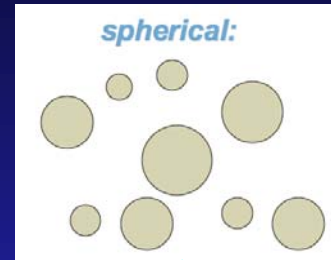
Volten et al.

Volten et al. 2001

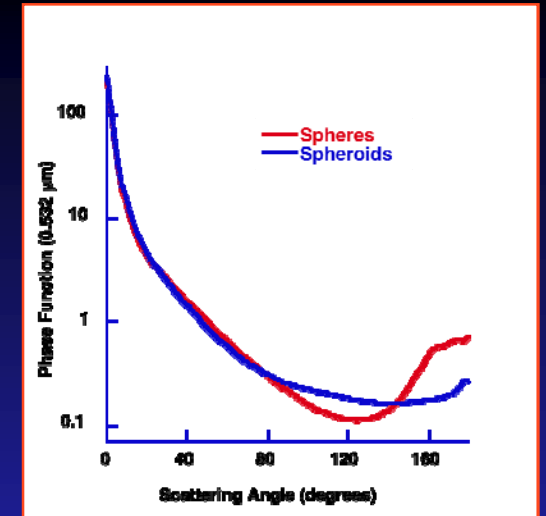


# Mixing of particle shapes retrieved

$C \times$



$+ (1-C) \times$



$$\tau(\lambda) = C \int_{r_{\min}}^{r_{\max}} K_{\tau}^{\text{spherical}}(k; n; r) V(r) dr + (1 - C) \int_{r_{\min}}^{r_{\max}} \left( \int_{\varepsilon_{\min}}^{\varepsilon_{\max}} K_{\tau}^{\varepsilon}(k; n; r, \varepsilon) N(\varepsilon) d\varepsilon \right) V(r) dr$$

Aspect ratio distr.

## ASSUMPTIONS:

- $dV/d\ln r$  - volume size distribution is the same for both components;
- non-spherical - mixture of randomly oriented polydisperse spheroids;
- aspect ratio distribution  $N(\varepsilon)$  is fixed to the retrieved by Dubovik et al. 2006